Materials Chemistry and Physics 341 (2025) 130878

Contents lists available at ScienceDirect

Materials Chemistry and Physics

journal homepage: www.elsevier.com/locate/matchemphys

Granulated activated carbon oxidation, a comparison between wet-chemistry and plasma approaches in dry and wet forms

Nathalie de la Torre-Miranda, Pierre Eloy, Eric M. Gaigneaux, Sophie Hermans *

Université Catholique de Louvain, Institut de la Matière Condensée et des Nanosciences (IMCN), Place Louis Pasteur 1, B-1348, Louvain-la-Neuve, Belgium

HIGHLIGHTS

- Active carbon was functionalized by wet-chemistry and Glid-Arc plasma.
- Direct exposition to plasma created carboxylic acids and high oxidation degree.
- Exposition to plasma in aqueous medium created phenols and a milder oxidation.
- The carbon's oxidation degree is independent of the plasma gas (O_2 or air).
- Glid-arc plasma gives high oxidation rates and low impact on textural features.

GRAPHICAL ABSTRACT

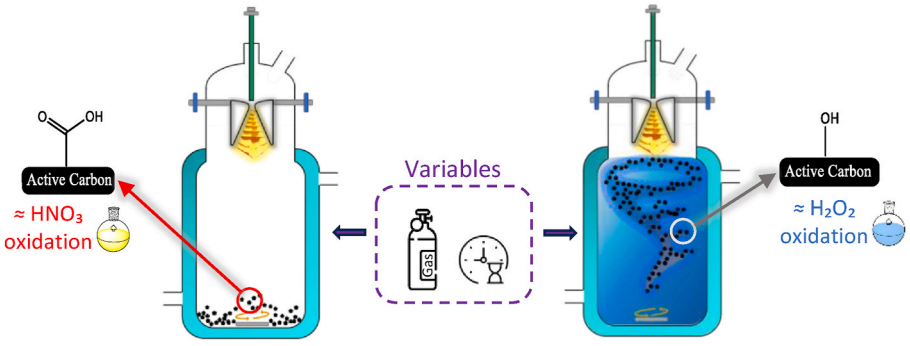

ARTICLE INFO

Keywords:
Activated carbon
Oxidation
Glidarc plasma
Wet-chemistry
Oxygen functional groups

ABSTRACT

Activated carbon oxidation was explored by comparing two approaches: wet-chemistry (employing HNO_3 or H_2O_2 solutions) and glidarc plasma exposure, working with different reactor configuration modes and gases. The oxidized samples were characterized by XPS, FTIR, N_2-physisorption, SEM, Boehm titrations and compared in terms of oxidation efficiency, created functionalities and morphological changes. Excellent oxidation is accomplished by exposing activated carbon in solid form directly to the plasma plume and the oxidized material shows characteristics similar to HNO_3 oxidized carbon: high oxidation degree with abundance of carboxylic acids. In contrast, if the carbon is exposed to plasma while being in water suspension, the oxidation degree is lower and the main created functions are phenols, with equivalent characteristics to H_2O_2 oxidized carbon. Additionally, it was demonstrated that the carbon's oxidation degree and type of oxygen functionalities seem little influenced by the type of gas used for plasma generation, though the presence/absence of water could enhance/diminish the nitrates or O–H containing species present in the oxidized carbons. Plasma oxidation has advantageously a lower impact on the carbon's textural properties than HNO_3 oxidation, while obtaining high oxidation efficiency, and the introduced oxygen functions seem stable for at least 6 weeks after plasma exposure.

* Corresponding author.
E-mail address: sophie.hermans@uclouvain.be (S. Hermans).

https://doi.org/10.1016/j.matchemphys.2025.130878
Received 28 January 2025; Received in revised form 4 April 2025; Accepted 14 April 2025
Available online 16 April 2025

1. Introduction

Activated carbon (AC) is the common name given to a type of highly porous carbon materials which are usually obtained from the carbonization of organic matter treated with oxidizing gases at high temperatures. They are employed in several fields for the removal of molecules or compounds from liquid and gas phases thanks to their high adsorption capacity. Indeed, the surface of this material is highly active and it can bind molecules physically (due to pi-pi stacking, for instance) or chemically thanks to the presence of the so-called "active sites", which are constituted by different functional groups grafted in the carbon's matrix. Between the different functional groups that could be present in activated carbons, oxygen groups are one of the most relevant ones [1–5].

In general, the presence of oxygen functional groups on the surface of carbon materials confers the solids several characteristics that permit their employment in a wide array of applications. For instance, oxidized carbons have been used in heavy metal water depollution, since it has been found that oxygen functions have chelating attributes that allow metal complexation in aqueous media [2,6,7]. Furthermore, by incorporating oxygen in the carbon's structure, the solid increases its polarity and often, it becomes more acidic [8–12]. Indeed, these oxygen groups can play the role of ion-exchange centers: while positively charged species could be electrostatically attracted to them, they could release protons to the solution, increasing its acidity [8]. Moreover, oxygen functions can be used as anchor groups for grafting other heteroatoms like N, S and P [13–15], transforming the carbon's surface in a flexible reaction platform [16], and opening its application possibilities even more broadly in the fields of environmental remediation, heterogeneous catalysts, electrochemistry, hydrogen storage and others [7,17].

Even if several oxygenated groups are present from the start in activated carbon, due to the natural source of raw material or activation procedure used to increase its porosity, several venues have been employed to further oxidize activated carbons. The most well-known ones are the dry and wet oxidation methods [2,5,18]. Dry oxidation methods incorporate oxygen in the carbon matrix by exposing the solid to oxidizing gases like water vapor, CO_2 or O_3 at high temperatures, usually above 700 °C [2,8]. In comparison, in wet oxidation methods, activated carbon is contacted with oxidant solutions like H_2O_2, HNO_3, NaOCl, $AgNO_3$, etc. at much lower temperature (usually boiling water or room temperature) [2,8,11,19]. The latter is the most commonly used approach for oxidation [8,20] since its application does not require expensive or sophisticated equipment and the needed reagents are common. Moreover, the targeted oxidation degree can be controlled by varying parameters like concentration, exposure time and temperature [5,11]. Nevertheless, these oxidizing agents could have a detrimental impact on the carbon's structure. For instance, it has been reported that HNO_3 oxidation could cause reduction of carbon's surface area and microporous volume due to pores walls collapsing and pore blockage [2,9,18]. Moreover, severe oxidation conditions could even cause the partial solubilization of the solid carbon, which is evidenced by the presence of humin substances after the oxidation process [5,8,9,21]. A milder alternative is employing H_2O_2 as oxidizing agent at room temperature. Nevertheless, high reagent consumption is needed to attain acceptable oxidation efficiency [5,22].

Plasma technology appears as an alternative and versatile tool to modify carbon materials in milder conditions than the common methods described above [23,24]. Plasma (considered as the 4th state of matter) is obtained when gases get excited by a source of energy, creating a cloud with a variety of highly reactive primary, secondary species, free radicals and protons, depending on the gas source [16,25]. When carbon is exposed to plasma, those species can penetrate several nanometers, breaking covalent bonds and getting its surface ready to react with other surrounding species, leading in that way, to the formation of new surface functional groups [16,26]. Furthermore, during this type of functionalization procedure, the bulk structure is not impacted and the burn-off is minimal, so the material could conserve important intrinsic characteristics like its mechanical strength [2,16,27].

In the case of carbon exposure to oxygen-containing plasmas, it is known that new oxygen functionalities such as carboxylic acid, lactones, peroxides and phenols groups could be introduced in the carbon's matrix [16,24,28]. Furthermore, the creation of these oxygen functionalities could be done in a rapid, solvent-free, dry way and the whole functionalization process could be achieved in few minutes, which compared to traditional dry and wet methods, represents an interesting competitive advantage [29]. For instance, Felten et al. [29] studied the functionalization of carbon nanotubes with an O_2 radio-frequency plasma and reported the formation of mainly carbonyl structures in the material. In another research, Boudou et al. [24] studied the modification of carbon fibers with oxygen microwave plasma, evidencing the enhancement of oxygen content in the treated material (principally due to the presence of carboxylic-type groups) and a decrease of the material's surface area due to plasma exposure, especially when the treatment was extended.

Regarding activated carbons, few studies have been devoted to their functionalization with plasmas and the literature found about this subject deals mainly with the oxidation of this material by their direct dry exposure to different type of dry oxygen plasmas. Among the previous works that could be mentioned, we can list the research of Huang et al. [30], who treated activated carbon fibers with O_2 low-temperature plasma for increasing its hydrophilicity. Additionally, the work of García et al. [27] suggests that activated carbon treatment with O_2 microwave plasma enriches the surface of the material with oxygen groups without altering the bulk structure, though the impact on the textural properties of activated carbons caused by plasma treatments is not clear yet, since it depends on the type of plasma and activated carbon employed for the functionalization process [5]. About granular activated carbon treatment with plasmas, Lee et al. [31] studied the functionalization of this type of carbon with a mixture of O_2 + He plasma produced by a dielectric barrier discharge equipment and they stated that the presence of He improves the uniformity of the functionalization. As far as we know, no research has been devoted to granular active carbon functionalization with air plasmas, neither the effect of water in the gas source has been assessed while oxidizing this type of carbon material.

Between the non-thermal plasmas that could be employed for material modification, Glidarc plasmas are one of the most interesting ones, due to their potential industrial use, versatility and scale-up possibilities. Indeed, Gliding arcs have been used industrially in different applications like air and soil depollution, plasmalysis of methane to produce H_2 and carbon black, CO_2 dissociation and others [23,32,33]. In Glidarc plasmas, the gas gets excited by passing through two electrodes connected to a high voltage generator [33]. This plasma is considered as a non-thermal plasma since the exposed object increases its temperature very moderately (few tens of degrees without cooling jacket), and therefore, it is suitable for treating even liquid solutions or suspensions [23]. Until now, this kind of plasma has been used for wastewater's treatment in batch or flow conditions, sterilization purposes, removal of VOCs, air and soil depollution, etc. [23,32,33]. In material sciences, it has been employed in clay functionalization [26], synthesis of MnO_2 nanoparticles for catalytic applications [34,35], and others. Literature reports about carbon materials functionalization with this type of plasma are very scarce, being the work of Chang Ming et al. [32] who modified activated carbon fibers by direct solid exposure to air plasma, the only report found about the topic, to the best of our knowledge.

In summary, due to the nature and specific operative characteristics of the plasmas that have been employed until now for carbons oxidation, the materials have always been oxidized through their direct exposure to the oxidizing plasma source, in small batches. As far as we know, never before other exposure ways have been tested, for instance, the possibility of oxidizing carbon materials by plasma while being in water suspension. This may be interesting to evaluate, not only from a

practical point of view, since this kind of exposure method may permit the functionalization of greater amounts of material in a possibly continuous way, which is relevant from a scale-up industrial perspective, but also from a fundamental point of view since the presence of water medium may have an impact on the plasma oxidation treatment and on the solid's oxidation characteristics, due to the presence of other reactive chemical species.

In this context, this research aims at exploring the functionalization of a coconut based granular active carbon with a Glidarc plasma. Thanks to the versatility of the Glidarc plasma system, two operating modes will be tested: the possibility of functionalizing the solid carbon grains by their direct exposure to the plasma plume in dry form and the effect of doing this functionalization while the carbon grains are suspended in water. Additionally, the influence of the selection of different gases (humidified or dry air/O_2) for generating the plasma plume will be assessed and the stability of the introduced oxidized functions will be determined. Furthermore, the same carbon will be functionalized by the traditional wet-chemistry approaches (through HNO_3 and H_2O_2 exposure) to compare the modified carbons in terms of surface functional groups composition, oxidation degrees and textural characteristics. For this purpose, the oxidized carbons will be characterized through different analytical techniques and methods including Differentiate Boehm Titrations, FTIR, XPS, N_2-physisorption analysis and SEM imaging.

2. Experimental

2.1. Materials and reagents

A granular, coconut shell-based commercial activated carbon (Calgon Carbon GRC 20/22, mesh 6 × 12 - ≈ 0.5 cm diameter grains - see Fig. A.4 in ESI) was used in all the functionalization tests. The following reagents were employed as received: nitric acid (HNO_3, 65 %, Roth), sodium hydroxide (NaOH, 99.2 %, VWR), hydrogen peroxide solution (H_2O_2, 35 %, Roth), air (α1, Air Liquide), argon (α1, Air Liquide), oxygen (α1, Air Liquide), sodium hydroxide standard solution (NaOH, 1 mol/L, Merck), sodium carbonate standard solution (Na_2CO_3, 0.05 mol/L, Merck), sodium bicarbonate ($NaHCO_3$, ≥99.7 %, Sigma Aldrich), hydrochloric acid (HCl, 37 %, VWR), potassium bromide (KBr, for spectrometric IR use, Roth) and deionized water.

2.2. Characterization methods and techniques

The oxidized samples' surfaces were characterized by X-ray photoelectron spectroscopy (XPS). For this purpose, a SSX 100/206 photoelectron spectrometer (Surface Science Instruments, USA) equipped with a monochromatized micro focused Al X-ray source (20 mA, 10 kV) was employed. For the analysis, activated carbon grains were fixed onto small brass troughs (Ø: 6 mm) with double-sided tape and arranged on a ceramic carousel, which was directly introduced into the analysis chamber, whose pressure was around 10^{-6} Pa. The analyzed area was around 1.4 mm^2 and the pass energy was fixed at 150 eV. The angle between the surface normal and the axis of the analyser lens was 55°. Under these conditions, the FWHM (full width measured at half maximum) of the Au $4f_{7/2}$ HR peak measured on a clean gold standard sample was about 1.6 eV. Charge stabilization was accomplished using a flood gun set at 8 eV and a Ni grid that was positioned 4 mm above the sample surface. The sequence of analyzed spectra was: survey spectrum, C 1s, O 1s, N 1s and C 1s again, to verify the charge compensation stability with time. CasaXPS program (Casa Software Ltd, UK) was used for data treatment. During data processing, the spectra were decomposed with the least squares fitting routine provided by the software with a Gaussian/Lorentzian (85/15) product function, after subtraction of a Shirley baseline. Normalised peak areas, based on acquisition parameters and sensitivity factors provided by the equipment's manufacturer, were used to calculate molar fractions. Data exploitation and peaks deconvolution methodology were based on the literature [70]. The samples were analyzed at least two times to assure repeatability. The total O content (Total O) of all the samples shown in Table 1 was quantified thanks to the deconvolution of O1s XPS high resolution peaks, while the O–C/Total C was calculated through the deconvolution and exploitation of the C 1s and O 1s high resolution peaks. 'Total C' corresponds to the whole C1s envelope, while the 'O–C' was calculated by summing up the contribution of the O bonded to C components found from 286.1±0.2 eV to 288.9±0.2 eV in the C 1s high resolution peak. A balance between computed and detected oxygen was done to corroborate that the assigned contributions were accurate.

The presence of oxygen functional groups in activated carbon was evidenced using Fourier transform infrared spectroscopy (FTIR) in transmission mode. For the analysis, a Bruker Alpha spectrometer equipped with DTGS detector was used. To avoid the interference of water and CO_2 in the spectra, the equipment was placed inside a globe box with controlled argon atmosphere. KBr pellets with a dilution rate of 0.5 wt % activated carbon were elaborated for the analysis. To prepare the pellets, KBr and activated carbon granules were both ground in a mortar and pestle until attaining a particle size <100 μm. The KBr-carbon mixture was pressed applying 10 tons and the obtained pellet was dried overnight under vacuum to remove water interference before carrying out the analysis. The spectra were obtained with 100 scans in the range of 800–4000 cm^{-1} with a resolution of 2 cm^{-1}. OPUS software version 7.5 was used for spectra exploitation and background correction.

A Micromeritics equipment model ASAP 2020 was employed for N_2-physisorption analysis of the functionalized and non-functionalized activated carbons. Before the analysis, the samples were outgassed under the following conditions: pressure <5 mmHg, evacuation phase: 90 °C during 1 h. Heating phase: 120 °C during 10 h. Nitrogen adsorption-desorption isotherms were obtained by dosing nitrogen at 77 K in the outgassed samples. The Brunauer-Emmett-Teller (BET) method applied in a low P/Po range (P/Po: ≈0.0001 to 0.06), as proposed by Rouquerol [36] for microporous materials, was employed to estimate the equivalent specific surface area of carbons. The material's external specific surface area was determined by the slope of the line drawn in the linear portion of the t-plot (calculated according to the Hakins and Jura method) in the 6.5–10.3 Å thickness range, according to experimental recommendations found in Ref. [37]. The microporous volume was determined by the intercept calculated in the same range. The difference between the BET equivalent surface area and the exterior surface area was used to estimate the micropores specific surface area of the analyzed carbons. The Density Functional Theory (DFT) method, presuming a slit pores' geometry, was used to determine the distribution of pores in the material.

A field-emission scanning electron microscope JEOL 7600F (15.0 kV, WD: ≈7 mm) was used for SEM analysis of the modified activated carbon samples. For the analysis, activated carbon grains were sticked on a 26 mm diameter specimen holder using a double-face tape and the sample was introduced in the analysis chamber without any additional treatment.

To evaluate the variation in carbon acidity resulting from functionalization treatments and the presence of oxygen functional groups, Differential Boehm Titrations were used as a key characterization method to quantify oxygen species and determine the degree of carbon oxidation. This methodology is explained in the literature in detail [38–40] and it is a reliable and straightforward technique to determine different oxygen species in carbon materials. During a typical experiment, 0.5 g of activated carbon grains was contacted under agitation with a basic solution (NaOH, Na_2CO_3 or $NaHCO_3$, molar concentration: 0.05 M) for 24h. Afterwards, the carbon was filtrated, and a 10 mL aliquot was taken and transferred to an erlenmeyer. Then, the aliquot was acidified by adding an exact amount of HCl solution (0.05 M): 20 ml of HCl was added if the contact base was NaOH or $NaHCO_3$, while 30 ml was added if the base was Na_2CO_3. Subsequently, this solution was

Table 1
XPS quantification of non-oxidized and oxidized samples by wet chemistry and plasma approaches.

Type of Treatment	Sample	XPS quantification					
		Total O (% at.)	O–C/Total C	NO_3^- & NO_2^- (% at.)	N^+-(C,H) (% at.)	N-(C,H) (% at.)	Total N (% at.)
Non-oxidized	Nox	8.6	0.09	0.7	0.0	0.0	0.7
Wet chemistry	Hox	15.8	0.23	0.7	0.3	0.3	1.3
	H_2O_2ox	13.2	0.18	0.2	0.2	0.3	0.8
Plasma (solid mode)	O_2Pl	15.0	0.17	0.9	0.2	0.3	1.4
	O_2.H_2O.Pl	18.8	0.19	0.8	0.1	0.3	1.3
	AirPl	15.2	0.16	1.0	0.2	0.3	1.5
	Air.H_2O.Pl	16.7	0.18	0.8	0.2	0.3	1.3

degassed by bubbling Ar for at least 2h to eliminate CO_2. Lastly, degassed NaOH (0.05 M) was used to titrate the degassed solution, employing phenolphthalein as indicator. Both NaOH and Na_2CO_3 solutions (0.05 M) were prepared by the direct dilution of commercial standards. HCl solution was prepared by dilution of concentrated HCl (37 %) in water and then, the obtained solution was standardized by titration with previously degassed NaOH standard solution, using phenolphthalein as indicator. Regarding the $NaHCO_3$ solution, it was prepared by dilution of solid reagent (≥99.7 %) in water. Afterwards, the solution was standardized by titration with previously standardized and degassed HCl solution, employing methyl orange as indicator. Boehm titrations were also used to determine basic functional groups in all oxidized carbons, implementing an inverse procedure compared to titration of acidic groups. In a typical procedure, 0.5 g of AC were put in contact for 24 h with 50 mL of HCl (0.05 M). Then, after filtration and degassing by Ar for at least 2 h, a 10 ml aliquot was titrated with a previously degassed NaOH (0.05 M) solution, using phenolphthalein as indicator.

2.3. Methods

Two approaches were used to oxidize activated carbon (AC): the wet chemistry approach (through HNO_3 and H_2O_2 solutions) and the Glidarc plasma oxidation approach.

2.3.1. Wet chemistry approach

2.3.1.1. HNO_3 oxidation. Activated carbon grains (4 g) were put in a round-bottom flask along with 250 mL of HNO_3 (2.5 M) for 6 h. The system was agitated and heated at 105 °C, under reflux, using a NaOH trap for acid vapors. Subsequently, the carbon was filtrated out, washed with plenty of deionized water (at least 2 L) and dried under vacuum for several hours. This oxidized carbon will be referred to hereinafter as Hox.

2.3.1.2. H_2O_2 oxidation. Activated carbon (4 g) was dispersed in 50 mL of H_2O_2 solution (35 %) and agitated at room temperature for 2 h. Then, 50 mL of fresh H_2O_2 solution was added to the reaction flask, and this procedure was repeated every 2 h, until completing a total period of 10 h (total H_2O_2 solution in contact with AC: 250 mL). After the contact time has passed, the solid was recovered by filtration and washed with plenty of deionized water. Finally, the sample was dried under vacuum overnight and stored. This oxidized activated carbon will be referred to as H_2O_2ox.

2.3.2. Plasma oxidation approach

2.3.2.1. Glidarc plasma reactor. A Glidarc plasma reactor was used for activated carbon oxidation. The design of the plasma reactor is based on an equipment described elsewhere [33,41]. It is composed of a glass doubled-wall reactor equipped with a water cooling system. The reactor has an upper head where two symmetric steel electrodes are fixed around a gas nozzle. The electrodes are connected to a high voltage generator (Siet, model 9000/120.4,5 kV, 100/120 mA) that will produce a discharge at the minimum distance between the electrodes. The plasma arc is generated when the gas passes through the discharge point, it glides along the electrodes and collapses at the end. Then, a new arc is immediately created and the process starts again, indefinitely. Before entering the reactor, the gas flow is controlled by a mass flow meter (Bronkhorst) and it could be humidified by passing through a bubbler full of distilled water. A scheme of this system is depicted in Fig. 1.

2.3.2.2. Activated carbon exposure mode to plasma. To oxidize activated carbon, the Glidarc plasma reactor was employed in two configuration modes: either by exposing activated carbon grains (1.5 g) directly to the plasma plume (distance between activated carbon grains and plasma plume: ≈11 cm) (named *solid mode*) or by suspending such grains in water (1 % solid) (named *suspension mode*). In both cases, the grains were agitated with a magnetic stirring bar and humidified oxygen was used to generate the plasma plume. The gas flow was maintained at 380 L/h. Several exposure durations were implemented, and the functionalized activated carbons were characterized to assess the oxidation degree of the material after the plasma exposure. In the *solid mode*, the oxidized carbon could be recovered from the plasma reactor immediately after treatment for its characterization, while in the *suspension mode*, the grains were separated from water by filtration and dried under vacuum for several hours before being analyzed. A scheme of both plasma reactor configurations can be seen in Fig. 2.

2.3.2.3. Influence of the type of gas for plasma generation in carbon oxidation. In another experiment, activated carbon (6 g) was oxidized in the *solid mode* using different types of gas sources for plasma generation. Oxygen, humidified oxygen, air and humidified air were tested. The time of treatment was 90 min for all the experiments and the gas flow was 380 L/h. After each treatment, activated carbon was directly recovered from the plasma reactor, characterized and stored. The plasma treated carbons will be named depending on the gas source used for plasma generation. Therefore, AC oxidized with: oxygen plasma will be referred to as O_2. Pl, humidified oxygen plasma will be named as O_2. H_2O.Pl, air plasma will be identified as Air. Pl and humidified air plasma will be named as Air. H_2O.Pl. Non-oxidized activated carbon (AC used as received) was characterized as well for comparison purposes. This carbon will be called Nox.

2.3.2.4. Stability tests of plasma oxidized carbons. The stability of the oxidized functions introduced by plasma in carbons was determined through Boehm titration characterization at different moments after the sample's functionalization process. In this experiment, activated carbon grains (6 g) were exposed to air humidified plasma in the *solid mode* for 90 min as described in point 2.3.2.3. Then, this carbon was stored in a desiccator (under air atmosphere, at room temperature) and characterized several times over a period of 6 weeks, to determine the variation on the carbon's acidity with time.

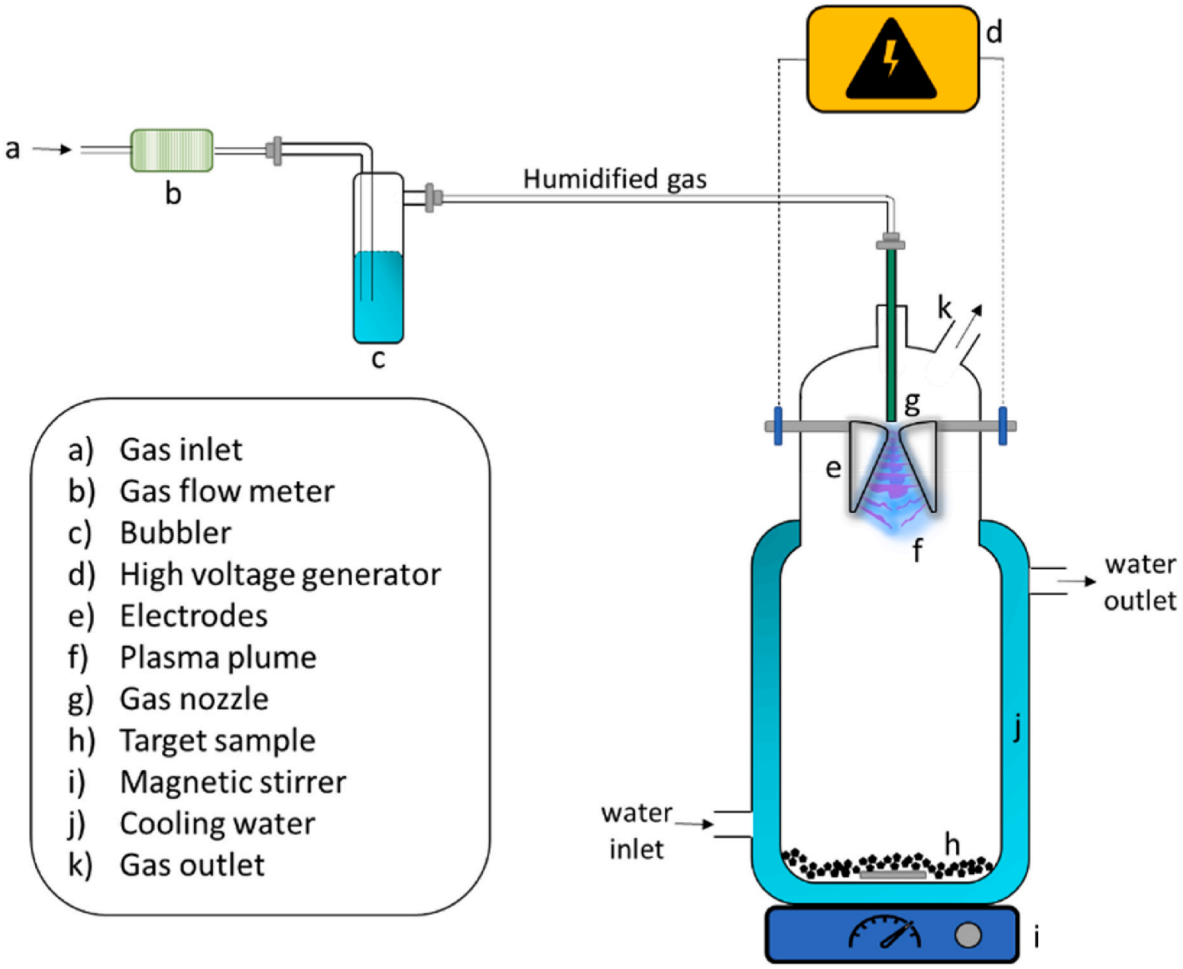

Fig. 1. Glidarc plasma reactor scheme.

3. Results and discussion

3.1. Wet-chemistry approach

The presence of oxygen functional groups created by wet oxidation treatments in the carbon matrix has been verified by Differentiate Boehm Titrations, FTIR and XPS. Fig. 3 shows the characterization of oxidized and non-oxidized carbons through Differentiate Boehm Titrations. As can be observed, both oxidizing agents have successfully increased the total acidity of the solid, which is in direct correlation with the presence of oxygen groups on the carbon's surface [42]. While the non-oxidized solid (Nox) has a low total acidity (8 mmol/100 g AC), after HNO_3 oxidation, the carbon increased its total acidity to 156 mmol/100 g AC. As expected, a milder oxidation is obtained employing H_2O_2 as oxidizing agent, attaining a total acidity of 77 mmol/100 g AC. Interestingly, different types of oxygen functionalities have been created depending on the used oxidant. While HNO_3 introduces mostly carboxylic acid groups, H_2O_2 enriches the carbon's surface mainly with phenol functionalities. Lactone groups are detected in lower quantities in both cases. This observation is in accordance with previous literature reports where carbon materials have been oxidized by these oxidizing agents [19,43–45]. No basicity (0 mmol/100 g AC) was found in any of the oxidized samples, while the pristine Nox carbon had 60 mmol/100 g AC of basic groups.

FTIR analysis of oxidized and non-oxidized carbons supports Differentiate Boehm Titration observations. Fig. 4 shows that new bands are detected in the oxidized carbons (Hox and H_2O_2ox), that were not present in the non-treated sample (Nox). Firstly, at ≈ 1720 cm^{-1}, a clearly defined band is observed in the sample Hox. This band could be assigned to the C═O stretching of the carbonyl group in carboxylic acids, lactones and ketones [18,46–48], which corroborates Boehm Titration quantifications, since this sample is rich in carboxylic acid functionalities. The same band appears weakly in H_2O_2ox, which is understandable since the oxidation of this AC is milder and the quantity of carboxylic acids and lactones is smaller compared to Hox. Secondly, a band at ≈ 1570 cm^{-1} could be distinguished in both oxidized samples. This band has been observed in other researches in oxidized samples and it has been attributed to C═C aromatic ring stretching vibration [47], highly conjugated C═O groups [46] or quinones [18,49]. Additionally, a sharp band at ≈ 1384 cm^{-1} is detected in both oxidized samples, but its intensity is higher in Hox. This band could be assigned to NO_3^- asymmetric stretching [48] and may indicate the existence of inorganic nitrates in Hox, which may be present due to HNO_3 residue that was not completely washed from the carbon's surface (trapped in the smallest pores) or NO_3^- and NO_2^- species that were incorporated in the carbon's matrix, since this phenomenon is known to occur in carbon materials oxidized by HNO_3 [9]. Regarding H_2O_2ox, this band may be present due to impurities of KBr (since it is known that KNO_3 could be present in KBr in small amounts as contamination) [48], or to possible impurities of the sample/reagent, since H_2O_2 cannot enrich carbon with N groups. Furthermore, an increase in intensity of a broad band between 1000 and 1200 cm^{-1} is observed in the oxidized carbons, compared to Nox. This band could be a contribution from several types of functional groups, including the C–O stretching in ethers, C–OH and O–H bend/stretching of phenolic groups and alcohols [18,47–49]. Besides, H_2O_2ox shows a band at ≈ 1260 cm^{-1} which could be attributed to the in-plane O–H

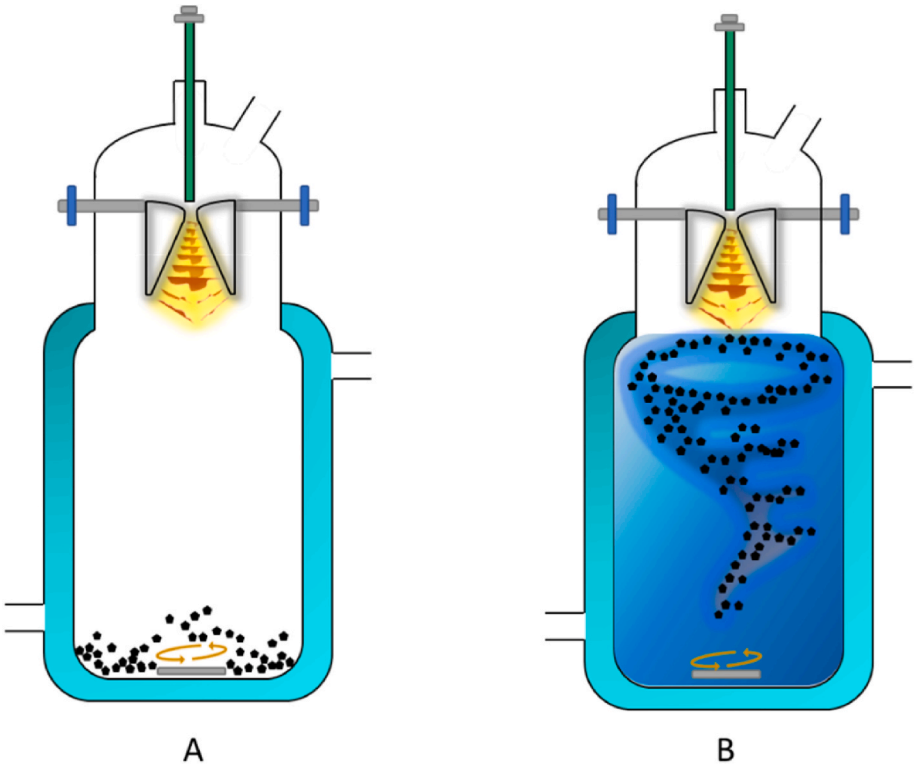

Fig. 2. Plasma reactor configuration: A) Solid mode. B) Suspension mode.

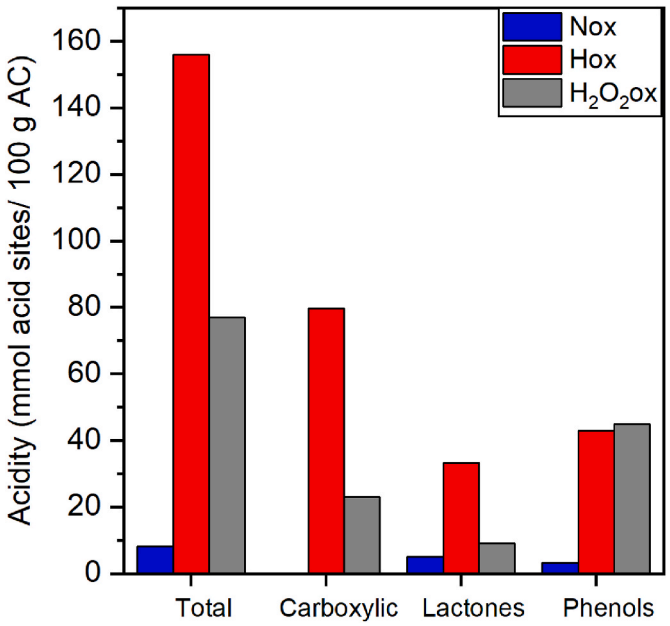

Fig. 3. Differentiate Boehm Titrations of non-oxidized (Nox), HNO_3 oxidized (Hox) and H_2O_2 oxidized (H_2O_2ox) activated carbons.

deformation vibration of alcohols [18,48], which corroborates what was observed in Boehm's characterization: H_2O_2ox is rich in phenolic groups. Lastly, all the samples present several small bands between 2850 and 2950 cm^{-1}. These bands may correspond to C–H vibrations of the carbon matrix or O–H groups [48].

The XPS quantification results of non-oxidized (Nox) and oxidized samples (Hox and H_2O_2ox) are shown in Table 1. Typical recorded O 1s and C 1s high resolution XPS peak are given in Supplementary Information (see Fig. A. 3.) and N 1s peaks can be observed in Fig. 5. XPS confirms the oxidation of the treated activated carbons: the oxygen content (column Total O) increased from 8.6 % at. (Nox) to 15.8 % at. and 13.2 % at. for the HNO_3 and H_2O_2 oxidized samples, respectively. This tendency is confirmed when comparing the ratio between oxygen linked to C to the total carbon detected in these samples (column O–C/Total C, which was obtained by the decomposition and quantification of the XPS C 1s HR peak). While this ratio in the non-oxidized sample corresponds to 0.09, in the oxidized ones, it is augmented to 0.23 (Hox) or 0.18 (H_2O_2ox), which confirms that the detected oxygen increment comes actually from oxygen groups linked to C. Additionally, HNO_3 treatment increases the total N content of the oxidized sample from 0.7 (Nox) to 1.3 % at (Hox). Moreover, by analyzing the N 1s HR peak of the latter sample (see Fig. 5B), it could be seen that HNO_3 oxidation introduces small amounts of new nitrogen species in carbon, which were not present in the non-oxidized one (notice that Nox contains just NO_3^- at BE: ≈406.7 eV [50,51], Fig. 5A). These new N species are detected at lower binding energies and could be attributed to N-(C,H) (BE: ≈399.6 eV [52]), which could be present due to the introduction of small amounts of N in the carbon matrix or due to HNO_3 non-washed residues in the carbon's pores and N^+-(C,H) (BE: ≈401.5 eV [53]), which may reflect a possible protonation of N species due to analysis conditions or to intrinsic surface protonated species [54]. Also, it is noticed that the peak located at the highest binding energy (pink peak at ≈ 405.6 eV in Fig. 5B) is found in a slightly lower position in Hox, compared to the same peak in Nox (Fig. 5A). This may mean that other forms of N oxidized species, such as C–NO_2 or NO_2^-, may exist in Hox, in addition to C–NO_3^- or NO_3^- species. Hence, this component may be a contribution of both nitrates and nitrites. These observations are in accordance with other researches, where the presence of NO_3^- and NO_2^- species were reported on HNO_3 oxidized carbons [9].

Nitrogen components at similar positions are observed in the H_2O_2 oxidized sample (Fig. 5C), though in even smaller quantities than in Hox (see Table 1). Actually, the total N content of H_2O_2ox (0.8 % at.) is really close to that in the starting Nox (0.7 % at.). Therefore, in this case, since H_2O_2 cannot enrich the carbon with N, these nitrogen species may

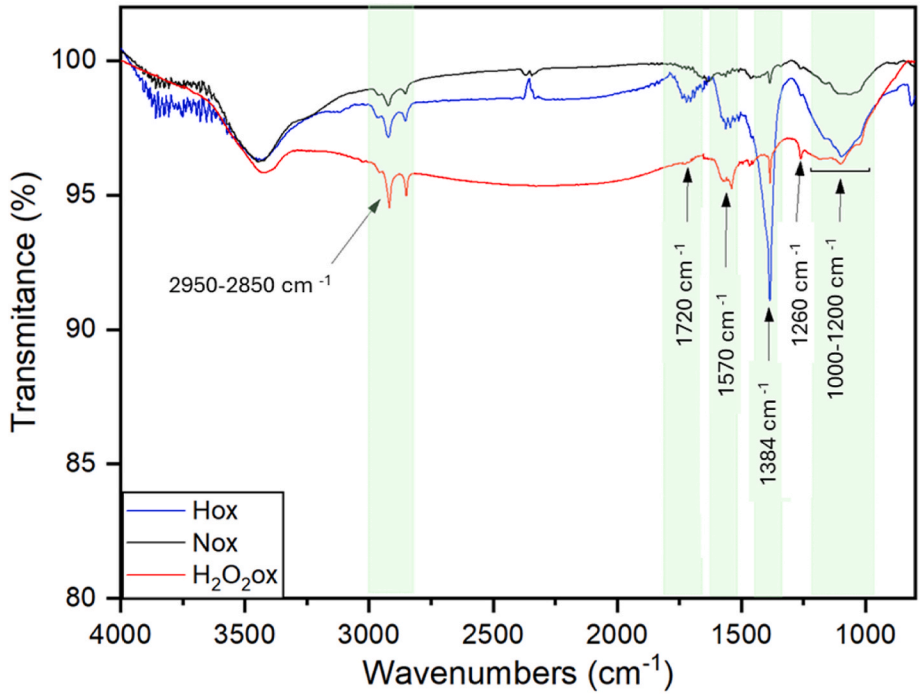

Fig. 4. FTIR analysis of non-functionalized (Nox), HNO_3 oxidized (Hox) and H_2O_2 oxidized (H_2O_2ox) activated carbons.

indicate traces impurities coming from the solid itself or the reagent (as was stated above in FTIR analysis). Nevertheless, it can be noticed that the nitrates' content (pink peak at BE ≈ 406.1 eV in Fig. 5C) has been reduced after the sample was contacted with H_2O_2, compared to the non-oxidized one, which may be due to the fact that some water-soluble nitrates salts may have been washed away after the oxidation process (remember that after treatment, the solid named H_2O_2ox was washed with plenty of water before being dried, stored and characterized).

3.2. Plasma approach

As stated above, activated carbon grains were functionalized in a Glidarc plasma reactor and the influence of several parameters on the carbon's oxidation were evaluated including: the mode in which activated carbon grains were exposed to the plasma plume (*solid mode* vs *suspension mode*) and the employment of different gases to generate the plasma plume such as dry/humidified air or O_2. Additionally, the stability of the created oxygen functions was assessed through the characterization of one sample during several weeks and the impact on the material's textural properties was assessed through SEM and physisorption analysis.

3.2.1. Exposure mode of activated carbon grains: solid mode vs suspension mode

Activated carbon grains were exposed to the plasma plume (employing humidified oxygen as plasma generating gas) in two ways named: *solid mode* (direct exposure to the plasma flame) and *suspension mode* (AC grains exposed to plasma while suspended in water). Fig. 6 shows the total acidity quantified by Boehm Titrations of the oxidized carbons after different exposure times. The *solid mode* was found to be the best way to accomplish a maximum oxidation of the material (205 mmol acid sites/100 g of active carbon) after 90 min of plasma treatment. Moreover, this exposure time was found to be the optimal one, since a decrease in total acidity (and therefore on the amount of oxygen functional groups) is evidenced if carbon is exposed for longer time (e.g. 120 min). This phenomenon has been observed by other authors before, while treating carbon fibers and polymers with oxygen plasmas for extended periods [24,55,56]. Indeed, they observed that the majority of oxygen species were incorporated in the plasma treated materials at initial stages of plasma treatment (at short exposure times) after which a "saturation" level is reached and the material cannot longer augment its oxidation degree. They reported that plasma functionalized materials could reach a "steady-state" condition in which the surface oxidation and the removal of the surface species by plasma reaches an equilibrium and the oxidation level cannot be increased any further. Indeed, plasma is known for its 'cleaning' effect on surfaces as well [20]. Hence, the material cannot longer increase its oxidation degree with longer plasma exposure time.

This is exactly what is evidenced while oxidizing AC in the *solid mode:* at just 30 min exposure, 51 % of the total acid sites accomplished at the optimal exposure time (corresponding to 105 mmol acid sites/100 g) are already present in the carbon. After this time, the increase of acidity is more gradual, reaching its maximum at 90 min. It has to be considered that plasma treatment functionalizes just the outermost surface layers of the carbon, due to the fact that the active plasma oxygen species need low activation energies to react with carbon atoms. Hence, these oxygen species may not be able to diffuse internally to react with carbon atoms located deeper within the carbon matrix [24,56]. Therefore, it could be inferred that at the optimal exposure time, the oxygen plasma species have already reacted with most of the available external carbon atoms, hence, the oxidation degree cannot go further. Considering that this sample's surface area measured by nitrogen physisorption analysis is around 982 m^2/g and that it contains 205 mmol of acid sites per 100 g of activated carbon (as determined by Boehm Titrations), we can calculate the density of O groups in the material at its optimal exposure time as a number of acid species per nm^2, which in this case, corresponds to 126 acid sites/100 nm^2. If we consider that one benzenic ring occupies an area of ≈16 $Å^2$ and consider that the oxidation could occur on all the carbon's surface area (≈982 m^2/g), it is estimated that each benzenic ring would present 0.2 acid sites, meaning that there should be some benzenic rings that do not contain oxygen species. These would contribute to keeping the general structure of the solid intact. Nevertheless, it is known that plasma cannot functionalize all the carbon's surface area, which is mainly of microporous character. In contrast, if we consider that plasma oxidizes just the external specific surface area of our activated carbon (≈14 m^2/g), we

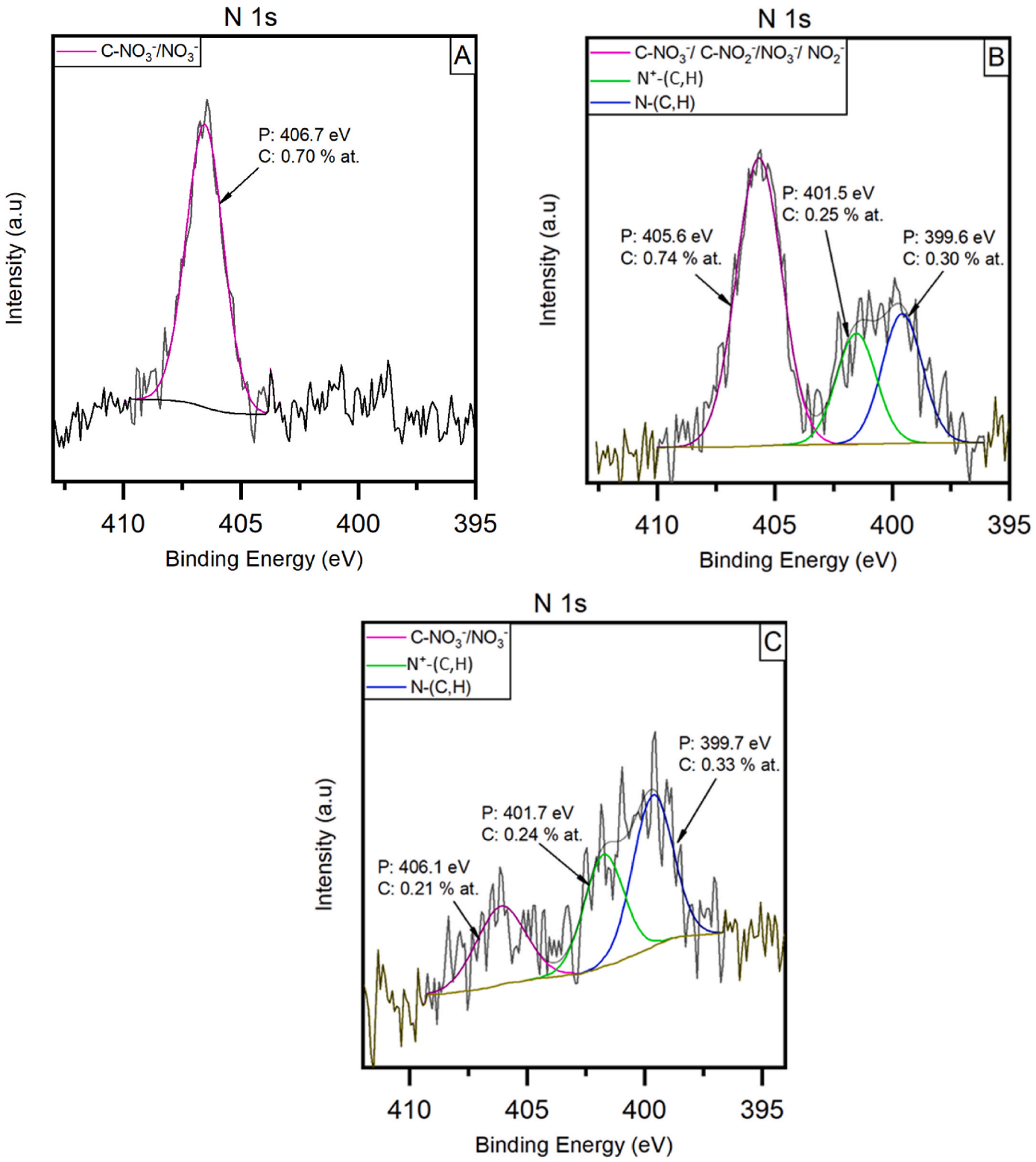

Fig. 5. N 1s XPS HR peak of: A) non-oxidized AC, Nox. B) HNO_3 oxidized AC, Hox. C) H_2O_2 oxidized AC, H_2O_2ox.

find out that every benzenic ring located on the external surface would contain around 14 acidic functions, which is unreasonable. Hence, based on this analysis, it could be inferred that plasma is functionalizing the carbon's external surface area and probably the entrance of its micropores, which according to Marsh and Rodriguez-Reinoso [4], are comparable to tree roots. For calculation details, refer to Annex A, Table A. 1.

Moreover, if after the saturation point has been reached (at 90 min exposure), the material is exposed to plasma for longer periods (e.g. 120 min), a removal of already incorporated oxygen species could happen probably due to the 'cleaning' effect of plasma and/or a deterioration of the carbon's structure. Similar behavior has been reported by Boudou et al. [57]. They observed that by exposing carbon fibers for extended periods to plasma, a reduction of oxygen content was evidenced due to a

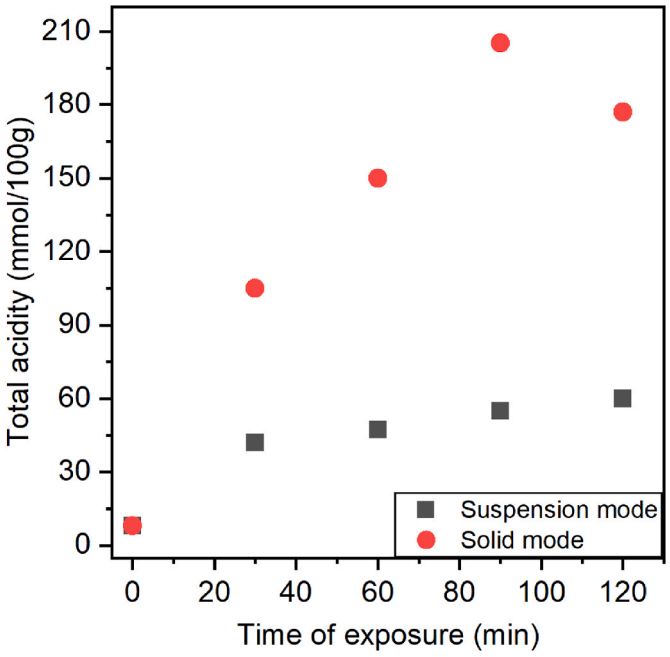

Fig. 6. Activated carbon's total acidity (determined by Boehm Titration) after functionalization with humidified oxygen plasma either in suspension or solid modes, at different exposure times.

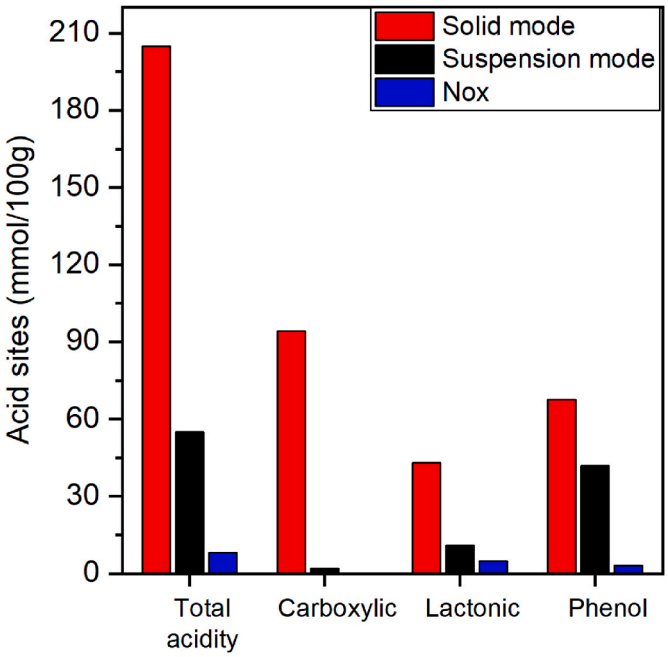

Fig. 7. Functional groups distribution in activated carbon exposed to humidified oxygen plasma for 90 min in the solid and suspension modes.

reduction of the material's microporous volume.

Regarding the carbon that was oxidized in the *suspension mode*, it could be observed that a lower functionalization degree is attained (60 mmol acid sites/100 g of active carbon after 120 min of plasma treatment). Furthermore, similarly to what happens to the material treated in the *solid mode*, the majority of oxygen functional groups are incorporated after 30 min exposure (70 % of the total acid sites obtained after 120 min exposure are already present after 30 min treatment), after which the increment in the acidity of the material is very slow. Nevertheless, in this oxidation mode, a decrease of acidity is not evidenced even after 120 min exposure, more likely because the "saturation" oxidation level was not reached yet (therefore, it could be assumed due to the tendency observed in Fig. 6, that if the carbon in suspension mode is oxidized for longer periods, the oxidation degree of this sample would increase). In this case, the density of O groups in the material (considering a SSA of 984 m^2/g) is 37 acid sites/100 nm^2, which is notably smaller than the 126 acid sites/100 nm^2 accomplished when oxidizing the material in the solid mode. Making a similar analysis as above, if we consider that plasma functionalizes all the carbon's SSA (≈984 m^2/g), 0.06 acid sites per benzenic ring is estimated, which is in agreement with a lower carbon's oxidation in this case. For calculation details, refer to Annex A, Table A. 1.

Differentiate Boehm Titrations were carried out to determine the nature of functional groups that were introduced in the oxidized activated carbons, while working under these two plasma exposure ways. As illustrated in Fig. 7, the distribution of oxidized functional groups found in both treated carbons is different: while in the *solid mode* the main functionality is carboxylic acid groups (which have been found as the most abundant functionality in other researches where carbons were treated by oxygen plasmas [57,58]), in *suspension mode*, this functional group is almost absent, being phenol groups, instead, the most abundant species. Lactones are present in both cases in lower quantities. No basicity (0 mmol/100 g AC) was found in any of the oxidized samples.

To complement this characterization, FTIR analysis was carried out on the plasma oxidized carbons. As can be observed in Fig. 8, both spectra show different bands: for instance, while the *solid mode* treated carbon presents a clearly defined band at ≈ 1720 cm^{-1}, this band is almost absent in the *suspension mode* functionalized carbon. This band has been assigned to the C═O stretching of the carbonyl group in carboxylic acids [18,48], which corroborates the abundance of this functional group in the *solid mode* treated sample. Additionally, both carbons present a band at ≈ 1570 cm^{-1}, which has been observed by other authors in oxidized samples due to the presence of highly conjugated C═O groups [46] or C═C aromatic ring stretching vibration [47]. Interestingly, a fine band at ≈1384 cm^{-1}, which has been assigned to NO_3^- stretching [48] is present in both samples but its intensity is much remarkable in the carbon oxidized in the *solid mode*. This suggests that the *solid mode* oxidized AC may have a higher content of nitrates. Moreover, the same sample shows a band at ≈830 cm^{-1}, which is not present in the *suspension mode* treated carbon, that could be attributed to the N–O bending vibration [48]. Finally, a small band at ≈1260 cm^{-1} is detected in the *suspension mode* treated carbon, which has been attributed to the in-plane O–H deformation vibration of alcohols [18,48], corroborating the presence of phenols or other O–H containing species in this sample.

If we compare the functional groups distribution quantified by Differentiate Boehm Titrations in the carbons oxidized through the wet-chemistry approach by HNO_3 or H_2O_2 (see Fig. 3) and the FTIR spectra of the same samples (Fig. 4) with the plasma treated carbons, it can be noticed that AC oxidized in the *solid mode* has similar characteristics to HNO_3 oxidized carbon (sample Hox), meaning high oxidation degree, abundance of carboxylic acids and more intense NO_3^- band (in FTIR spectrum, band at ≈1384 cm^{-1}). In contrast, AC oxidized in the *suspension mode* is comparable to H_2O_2 oxidized carbon (sample H_2O_2ox), since it shows a low oxidation degree characterized by the presence of predominantly phenol groups. Several reasons may explain these characteristics in the plasma oxidized samples. Let's examine first the carbon that was oxidized in *suspension mode,* where AC grains were immersed in water. It has been reported in the literature that one of the most abundant reactive oxygen species present in oxygen-containing Glidarc plasmas is the hydroxyl radical °OH [23,59]. This radical, characterized by a high oxidation potential, has short living time and it is fleetingly formed in the arc zone [23]. Hence, it may not be able to oxidize the material, directly. Nevertheless, it can recombine forming other oxidative species like the dimer H_2O_2, which is highly soluble in water and

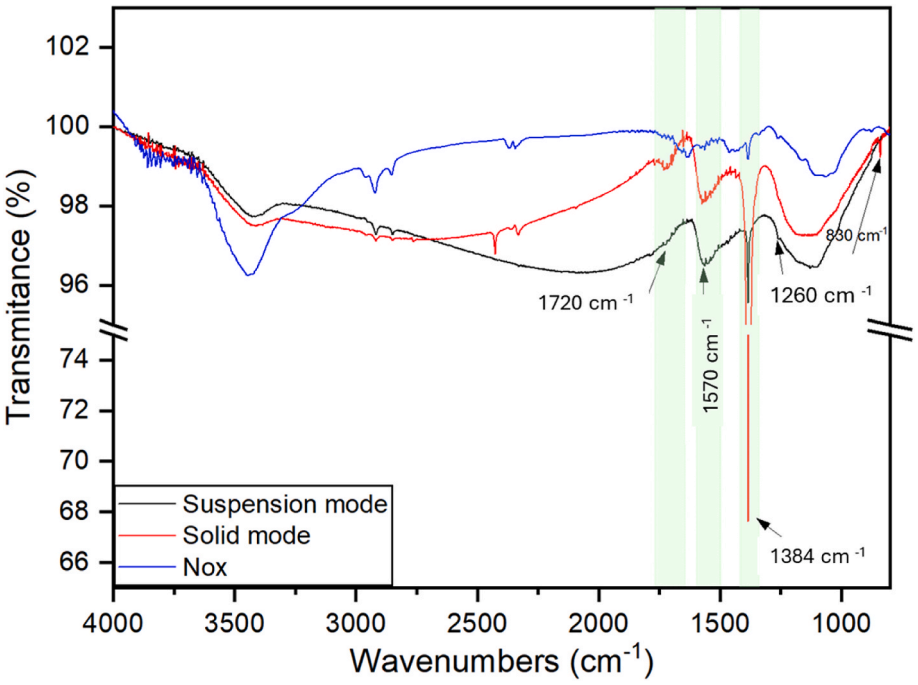

Fig. 8. FTIR analysis of activated carbon treated with oxygen humidified plasma in suspension and solid modes.

that could interact with the exposed material in *suspension mode* [23,59,60]. Moreover, the formation of H_2O_2 has been demonstrated in GlidArc plasmas [71] and several studies have demonstrated the presence of H_2O_2 species in aqueous solutions exposed to Glidarc plasmas by a colorimetric method [60–62], whose concentration tends to be higher if the gas is humidified, due to the fact that °OH radicals are commonly formed by the dissociation of H_2O [59]. Therefore, what may be happening in the *suspension mode* treated AC is that H_2O_2 is formed when the plasma reactive species touches the water surface, and it is this species the one that is finally oxidizing the solid, in a mild manner, forming mainly phenol groups.

By contrast, regarding the carbon that was treated in the *solid mode*, where activated carbon grains were directly exposed to the plasma plume, H_2O_2 may not be the main oxidative species, since the amount of water present in the system is considerably smaller (coming just from the humidification of the gas) and therefore, the amount of H_2O_2 formed by the recombination of hydroxyl radicals may be as well reduced. In this case, one of the probable reasons for the oxidation of the material may be the formation of nitric oxide NO (that is unstable and may be present just in the arc zone), which would rapidly oxidize to nitrogen dioxide (NO_2), which in turn will react with the hydroxyl, hydroperoxyl radicals or others (formed due to the presence of water in the gas) producing, ultimately, HNO_3 species. NO_2 may as well directly oxidize forming nitrates (NO_3) [23,59–61]. Some of the reactions occurring due to plasma exposure and that may help to describe these phenomena are shown below [23]:

Some reactions leading to the formation of NO°

$$N_2 + O^\circ \rightarrow NO^\circ + N^\circ \quad (1)$$

$$N^\circ + O_2 \rightarrow NO^\circ + O^\circ \quad (2)$$

$$N^\circ + O^\circ \rightarrow NO^\circ \quad (3)$$

Some reactions leading to the formation of NO_2

$$2\,NO^\circ + O_2 \rightarrow 2\,NO_2 \quad (4)$$

$$NO^\circ + O_3 \rightarrow NO_2 + O_2 + h\nu \quad (5)$$

$$NO^\circ + HO_2^\circ \rightarrow {}^\circOH + NO_2 \quad (6)$$

Some reactions leading to the formation of NO_3 and ultimately HNO_3

$$2\,NO_2 + O_2 \rightarrow 2\,NO_3 \quad (7)$$

$$NO_2 + O_3 \rightarrow NO_3^\circ + O_2 \quad (8)$$

$$H_2O_2 + NO_2^- \rightarrow ONOO^- + H_2O \quad (9)$$

$$NO^\circ + HO_2 \rightarrow ONOOH \quad (10)$$

$$NO_2 + {}^\circOH \rightarrow ONOOH \quad (11)$$

This hypothesis is supported by FTIR analysis done on the plasma oxidized carbons (see Fig. 8), since the *solid mode* treated carbon seems to have a considerably higher amount of nitrates than the one treated in *suspension mode*, judging for the notable difference of intensities of the band at 1384 cm^{-1}. It is important to remark that even though the gas used to generate the plasma plume was humidified oxygen, the reactor was opened to the air and undoubtedly, some air (and therefore N_2) should be present inside activated carbon's pores. Therefore, it is plausible that nitrogen from the air present in the reactor, may have interacted forming NO species under plasma exposure. In fact, nitrates have been observed by other authors in oxygen humidified Glidarc plasma treated samples and their formation have been attributed to air present in the reactor [60,61]. Moreover, Burlica et al. [61] and Porter et al. [60], who quantified the amount of NO_3 and H_2O_2 generated by Glidarc plasmas in aqueous solutions, found out that when the amount of nitrates detected in the exposed solution was high, a low concentration of H_2O_2 was quantified, because H_2O_2 will likely react with NO_2 species forming NO_3, according to Reaction 12 [23,61], and therefore H_2O_2 species may be suppressed and their concentration diminished. In summary, even though H_2O_2 may be formed thanks to H_2O present in the gas in small quantities, these H_2O_2 species may transform to NO_3^- and therefore, they may not be able to oxidize the material in the solid mode configuration.

$$NO_2^- + H_2O_2 \rightarrow NO_3^- + H_2O \quad (12)$$

Since the highest oxidation efficiency were obtained by working in the "*solid mode*" at 90 min exposure, this configuration and time of

treatment were conserved for further experiments.

3.2.2. *Influence of the type of gas for plasma generation in activated carbon oxidation*

Aiming to determine the influence of the type of gas used for plasma generation in activated carbon's oxidation efficiency and nature of oxygen functionalities, some experiments were conducted by changing the gas source for plasma generation. Fig. 9 shows the total acid sites quantified in these oxidized samples by Differentiate Boehm Titrations. Excellent oxidation efficiency are obtained employing all the tested gases, though a slightly highest total acidity is found in the sample that received treatment with air humidified plasma (sample Air. H_2O.Pl). Regarding the type of oxygen functionalities, the most abundant oxygen group in all the samples is carboxylic acids, followed by phenols and lactones, in lesser amounts. Additionally, when oxygen is used as oxidizing gas, the presence of water seems not to influence the oxidation degree of the sample, since the total acidity quantified in O_2. Pl and O_2. H_2O.Pl carbons is really similar. In comparison, the presence of water when air is used for plasma generation seems to enhance slightly the acidity of the sample.

Differently to what may have been expected, working with pure oxygen does not generate higher oxidation efficiency in the treated activated carbons. This may be due to the fact that plasma active oxygen species would interact mainly with the most outer-layers of the carbon matrix [57] until reaching the "saturation" point [56,57,63], as explained above. Therefore, even though the concentration of oxygen species may be higher in pure oxygen plasmas, the amount of external carbon atoms available to react is limited. Hence, the oxidation degree of the material could not be improved further. Also, it is interesting to notice that despite the highest concentration of N_2 in air plasmas (78 % compared to small amounts in oxygen plasmas, e.g. N_2 found in carbon pores), the total nitrogen content in all plasma exposed samples is comparable. This may be due to the lower reactivity of nitrogen compared to oxygen. Additionally, since the carbon is agitated with magnetic stirring bar through all the time that it was exposed to plasma

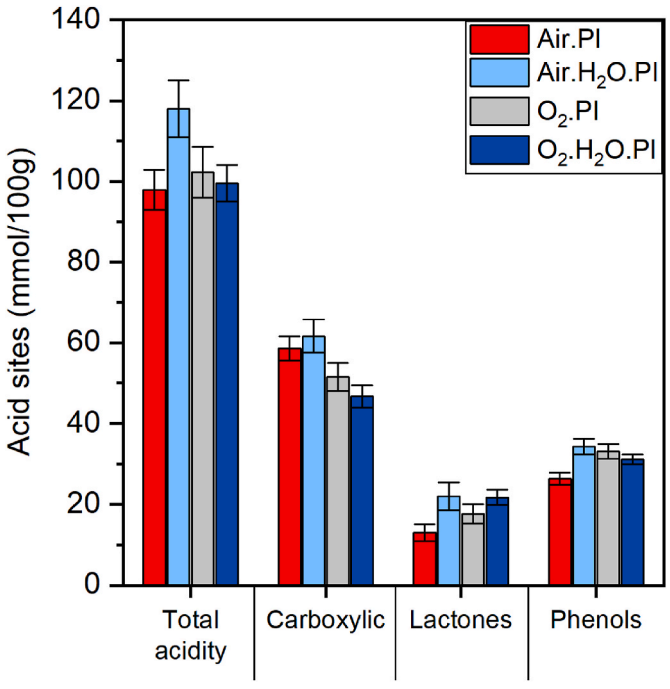

Fig. 9. Total acid sites and functional groups distribution of plasma oxidized samples using different gas sources. Time of exposure: 90 min. AC: 6 g. Reactor configuration: solid mode. The standard deviations shown in this graph have been calculated between samples of the same type, synthetized and measured at different moments. Error bars calculated from N = 2.

in all cases, being in suspension or dry forms, we can consider that all the carbon faces have been exposed to plasma, and hence, functionalized. This can be corroborated through the small standard deviation seen in Boehm titrations for all the samples: The functionalization process is uniform.

FTIR analysis was done on these four oxidized samples to determine the type of oxygen species introduced by plasma treatments. Fig. 10 shows the FTIR spectra of the samples oxidized by different plasma gas sources. All the treated samples present some common bands including the band at ≈ 1720 cm^{-1}, assigned to the C═O stretching of carbonyl groups taking part in carboxylic acids, lactones and ketones [18,46–48]. This observation is in accordance with Boehm titration results that evidenced carboxylic acid as the most abundant functionality in all these oxidized samples. Additionally, a band at ≈ 1570 cm^{-1} is seen in all the samples, which could be attributed to C═C aromatic ring stretching vibration [47], highly conjugated C═O groups [46] or quinones [18, 49]. Interestingly, a thin band at ≈ 1384 cm^{-1} denoting the presence of NO_3^- [48] is detected in all the oxidized carbons. Nevertheless, it is more intense in the samples that were treated with dry gases (O_2. Pl and Air. Pl). These samples contain as well a small peak at ≈ 830 cm^{-1}, attributed to the N–O bending vibration [48], which is not seen in the samples oxidized by humidified gases (Air.H_2O.Pl and O_2.H_2O.Pl).

Moreover, the carbons treated with humidified gas plasmas present several bands that have been assigned to O–H containing groups like the bands at ≈ 1260 cm^{-1} (O–H deformation vibration [18,48]) and at ≈ 1464 cm^{-1} (O–H stretching [45]), which is detected exclusively in these samples. Furthermore, it could be noticed that the large band at 3300-3550 cm^{-1} (assigned to O–H stretching [45,48]) and the multiple bands at ≈ 2850-3000 cm^{-1} (attributed to C–H and O–H stretching [48]) are notably enhanced in the same samples, compared to the ones treated with dry gases plasma. This fact could evidence that these carbons may not only present oxidized groups containing O–H functions bonded to C atoms (like phenols, carboxylic acids, etc.), but also probably, some O–H containing plasma secondary species like °OH(H_2O)n, H_2O_2, °O_2H, which may have been formed due to °OH radicals recombination [23, 25] and that may have remained on the carbon's surface after plasma exposure to humidified gases. Note that the amount of oxygen functional groups determined by Boehm titrations is really similar between all these oxidized samples, nevertheless, the ones that were exposed to humidified gases show more intense O–H bands, hence there should be an additional contribution of O–H species not coming from oxygen functional groups bonded to C.

In conclusion, the two samples that were oxidized by dry gases show a high intensity nitrate peak (band at ≈ 1384 cm^{-1}) and at the same time, weaker bands assigned to O–H species (bands at: ≈3300-3550 cm^{-1}, 2850-3000 cm^{-1}, ≈1464 cm^{-1} and 1260 cm^{-1}). In contrast, the samples oxidized by humidified gases contain a smaller nitrate band but stronger O–H assigned peaks, as mentioned above. This could be explained by two reasons: 1) the amount of O–H species would be less important in the samples oxidized by dry gases because these species will be mainly generated due to the decomposition of H_2O in the plasma plume [23] and 2) The O–H species (mainly H_2O_2) that may still be generated when using dry gases (because of the humidity of the environment for instance, since the reactor is opened to ambient air) will be transformed to NO_3^- following Reaction 12 [60,61] (see above), so its amount may be diminished even more. In other words, samples oxidized by dry gases show more N contents because these samples may contain HNO_3 species generated by plasma and maybe other NO_3^- species that come from the transformation of H_2O_2.

Finally, it is important to remark that the spectra of the carbons functionalized by humidified gases are really similar between each other. The same observation could be done for the samples that received treatment with dry gases. This provides further evidence that an enhanced oxygen concentration in the gas that generates the plasma plume seems not to have a significant impact on the chemical characteristics of the obtained oxidized solids, as seems to have instead, the

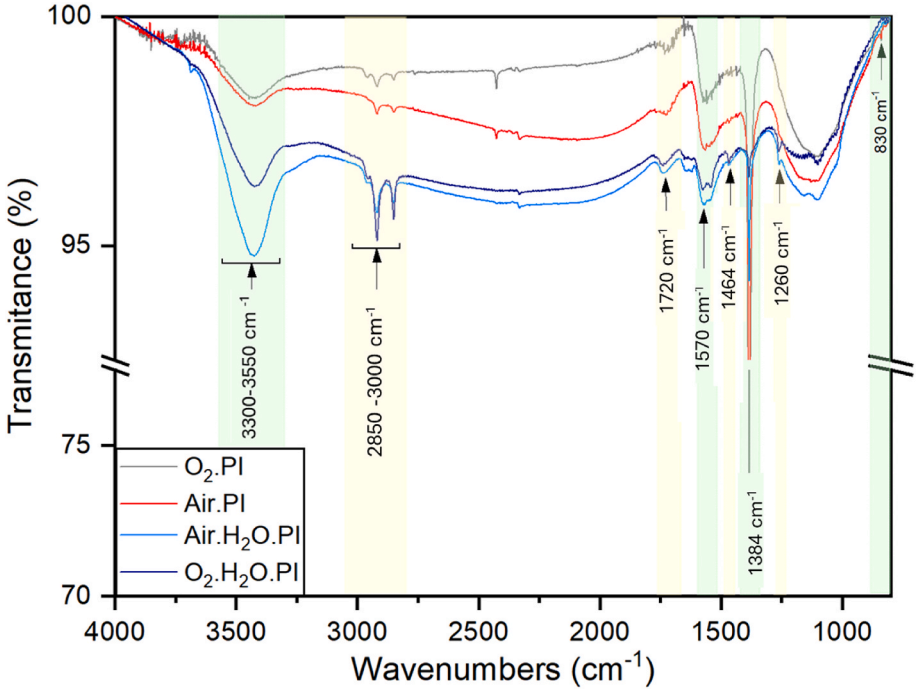

Fig. 10. FTIR analysis of plasma oxidized carbons with different gas sources.

presence of water in the gas source.

XPS analysis was carried out on the four oxidized samples to complement FTIR observations. As seen in Table 1, plasma exposure increased the oxygen content (see column Total O % at.) in all these oxidized samples, compared to the non-oxidized one (Nox). Typical O 1s and C 1s high resolution XPS peaks can be observed in Supplementary Information (see Fig. A. 3.). Moreover, an increment in the oxygen bonded to carbon ratio (column O–C/total C) is corroborated as well, which means that new oxygen functional groups bonded to the carbon matrix were indeed created thanks to plasma treatment. Nevertheless, notice that the samples that were treated with humidified gases plasmas (O_2.H_2O.Pl and Air. H_2O.Pl) contain the highest oxygen contents (column Total O) of all the samples' series (even higher than Hox which has the most elevated acidity, according to Boehm titrations), which is not necessarily reflected in a bigger O–C/Total C ratio (notice that all the plasma oxidized samples have similar O–C/Total C ratio, all lower than Hox, which verifies that the amount of oxygen species linked to C atoms is similar between them, as quantified by Boehm titrations). This brings additional evidence that the carbons oxidized with humidified gases plasma contain an additional oxygen contribution that does not come from oxygen functional groups linked to carbon and that may probably come from O–H containing plasma secondary species that are still present in the carbon after its exposure, as hypothesized above due to the enhanced O–H FTIR bands in these samples.

Additionally, plasma exposure enriched the samples with different nitrogen species, as the Total N content in all the plasma oxidized AC appears higher than the amount quantified in the non-oxidized one (Nox). Moreover, if comparing the samples oxidized by dry (O_2. Pl and Air. Pl) and humidified gases (O_2.H_2O.Pl and Air. H_2O.Pl), it can be evidenced that the nitrates/nitrite content (% at.) is indeed higher in the samples oxidized with dry gases (see column NO_3^- & NO_2^-), as also seen by FTIR. Also, this N component is the most important one in all the plasma oxidized samples. Finally, by analyzing the N 1s HR peak of these oxidized carbons (Fig. 11), it was determined that small amounts of other nitrogen functionalities located at lower binding energies were introduced by plasma treatments with all the tested gases: N-(C,H) at BE: ≈399 eV, that could be attributed to amines/amides [64] and N^+-(C,H) at BE: ≈401 eV, that is a protonated component that could denote the presence of quaternary amines or a protonation of amines due to analysis conditions or to intrinsic surface protonated species [53]. These nitrogen species appear at similar concentrations and positions in all the plasma-oxidized samples. Due to the notable presence of N species in the plasma oxidized carbons in general, and to the fact that HNO_3 plasma generated species may be the main oxidizing agent acting in these plasma exposed carbons, it could be inferred that nitrogen (either coming from ambient air or from the plasma generating gas itself) plays an important role in the plasma oxidation mechanism, which should be further studied. Finally, it can be considered that plasma functionalization is most likely to occur within at least 10 nm of the activated carbon grains' surface, since this is the analysis depth of XPS and most probably, the carbon bulk would not be functionalized. Nevertheless, this is not a problem as most applications would occur at the interface of these functionalized granules.

3.2.3. *Stability of the oxidized functions introduced by plasma treatment*

Since previous literature studies have reported that plasma oxidized activated carbons could change their chemical composition with time due to aging processes and possible post-reactions after plasma exposure (for instance, it has been reported that plasma oxidized carbons could increase their oxidation with time due to interactions of the carbon with oxygen in air) [20,57], one plasma oxidized carbon (reactor configuration: *solid mode*, time of exposure: 90 min, gas source: air humidified) was analyzed by Boehm titrations at several moments over a period of 6 weeks. Assessing the sample's total acidity variation in time may permit to determine the possible loss or incorporation of oxygen functional groups. Fig. 12 shows the total acidity of the plasma oxidized sample determined at several times after plasma exposure The sample's acidity does not experience a statistically significant change over time, even 6 weeks after its treatment. All the tested points are within the experimental error band for this type of sample. Hence, it could be stated that the oxygen functions introduced by plasma treatment seem stable for the tested period and no new oxygen groups seem to have been incorporated or lost within the sample due to aging processes.

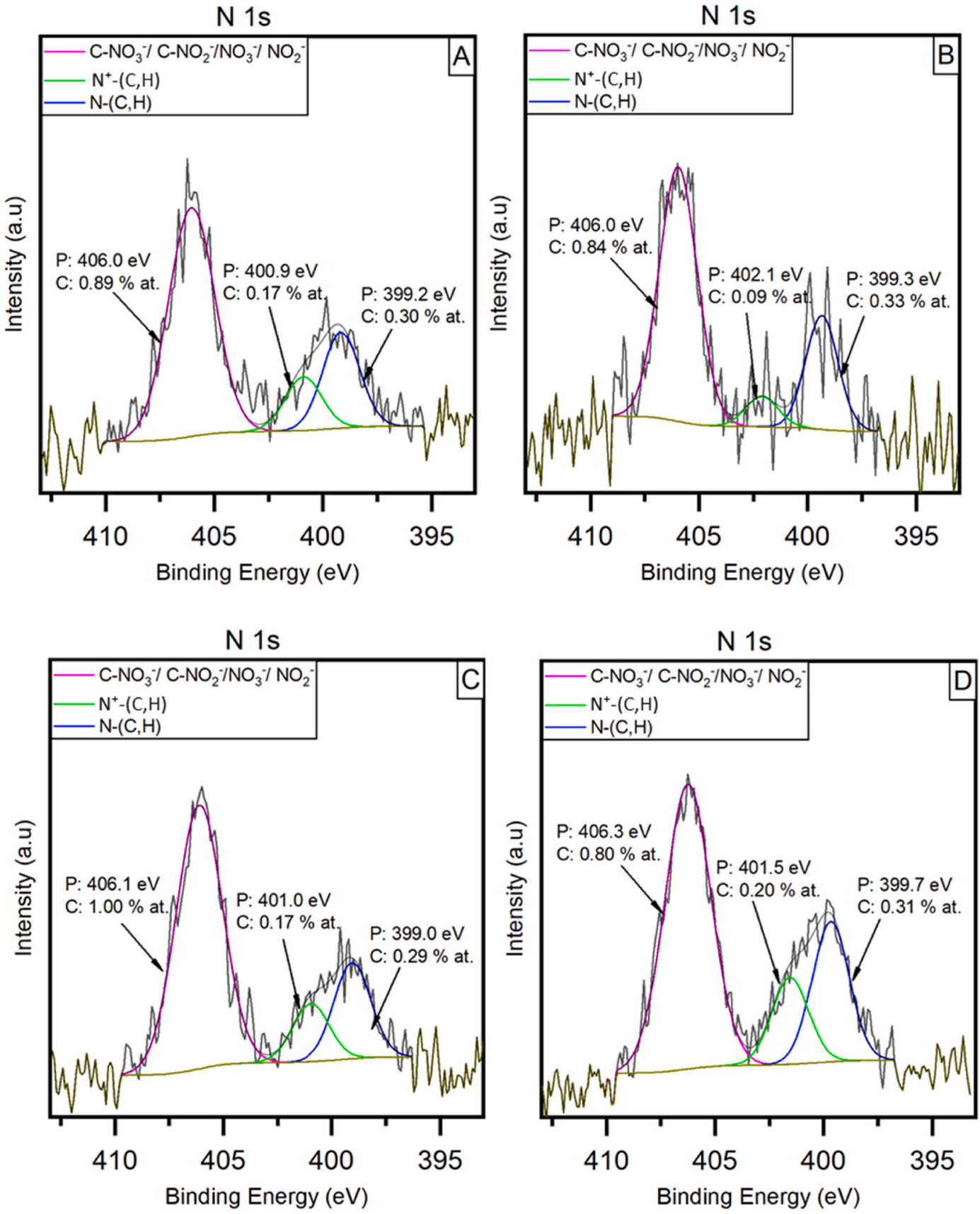

Fig. 11. N 1s HR XPS peaks of plasma oxidized samples with different gas sources: A) O_2. Pl, B) O_2.H_2O.Pl, C) Air. Pl, D) Air. H_2O.Pl.

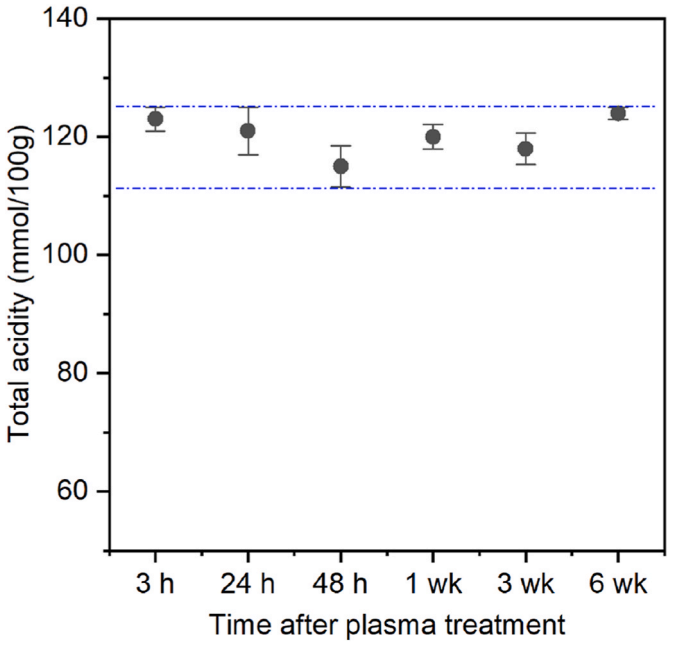

Fig. 12. Boehm titrations carried out at different times after plasma exposure. Oxidation conditions: reactor configuration: *solid mode*, AC: 6 g, gas source: air humidified, time of exposure: 90 min. In the graph, error barrs expressed with the dotted line (symbol ·····) have been calculated by oxidizing AC with plasma under the same conditions 2 times and characterizing the samples with Boehm method (two titrations of the same sample). Error barrs expressed by ⊥ were calculated by taking one sample of the plasma oxidized carbon at an specific time after plasma oxidation (eg. 3 h, 6 wk) and characterizing it two times by Boehm titrations.

3.2.4. *Changes in the carbon's surface area and texture due to oxidation treatments*

Activated carbons are known for their elevated specific surface area and a well-developed microporous system. These physical characteristics could play an important role in the adsorption capacity of the solid, depending on its application [1,4]. Nevertheless, it has been reported that oxidation processes, despite being beneficial in terms of heteroatoms' surface enrichment, could significantly modify the textural properties of the material, reducing its surface area and its microporous volume [2,65]. For instance, several authors have reported that acid treatments with nitric and sulfuric acids could reduce the total specific surface area of the solid by up to 33 %, depending on the oxidation conditions, due to micropores obstruction, collapsing and widening [2,65–67]. In contrast, plasma has been stated to cause a "milder" modification in the structure of treated carbon materials [20,57,68]. For instance, it has been observed that no damage was caused when exposing carbon nanotubes to O_2, Ar, H_2 and N_2 plasmas [20,68] and that an increase of rugosity and etching was evidenced when exposing carbon fibers to O_2 or air plasmas [32,57]. About granular activated carbon physical modification after Glidarc plasma oxidation, no previous literature reports have been found. For this reason, we have analyzed our oxidized activated carbon by N_2-physisorption and SEM analysis, to compare the possible physical morphological alterations that the solid may have experienced due to the different oxidation approaches. For this study, we have chosen the most oxidized carbons of each type of functionalization method: nitric acid oxidized AC (Hox) and air humidified plasma oxidized AC exposed in a *solid mode* reactor configuration (Air.H_2O.Pl). Non-oxidized carbon (Nox) was analyzed as well for comparison purposes.

The N_2-physisorption analysis results of different activated carbons are shown in Table 2. The non-oxidized activated carbon (Nox) possesses a high specific surface area (1066 m^2/g), thanks to its extensive microporosity (1053 m^2/g), along with a small external surface area (13 m^2/g). Nevertheless, after nitric acid oxidation, its specific surface area is reduced by about 13 % (927 m^2/g), with an evident drop of its microporous surface area and microporous volume, while its external surface area seems really similar to Nox. In contrast, when AC is oxidized by plasma, a milder impact on its physical properties is noted. Indeed, the specific surface of the material is reduced by 8 % (to reach 982 m^2/g), mainly due to a diminution of its microporous surface area and microporous volume (though in a lesser magnitude than in HNO_3 oxidized sample), while the external surface area is again really similar to Nox. As a complement, Annex A, Fig. A.1 shows the N_2 adsorption-desorption isotherms of the three samples, where a mixed type I and IV adsorption isotherm with H4 hysteresis is evidenced for all of them, which is generally observed in microporous adsorbents constituted by connected sheets, where capillary condensation could occur, which is in accordance with the known structure of activated carbons [37,69] and the presence of mesopores between highly microporous domains.

Table 2
Physisorption analysis of non-functionalized (Blank) and oxidized activated carbons by wet chemistry and plasma treatments.

Sample	BET equivalent specific surface area (m^2/g)	Microporous surface area (m^2/g)	Microporous volume (cm^3/g)	External surface area (m^2/g)
Nox	1066	1053	0.40	13
Hox	927	912	0.36	15
Air. H_2O. Pl	982	968	0.38	14

Furthermore, Fig. 13 shows the pores' distribution of the analyzed samples determined by the DFT model. As can be observed, the non-oxidized sample (Nox) presents smaller pores than the oxidized ones. Indeed, while the maximum pores' width is estimated at ≈ 20 Å for Nox, HNO_3 and plasma oxidized carbons present maximum pore's widths of ≈30 Å and 32 Å, respectively. Moreover, the three samples show a notable pores' region in the range of 13.6–17.2 Å, and a second pores' region from ≈17.2 to 30 Å is observed just in the oxidized carbons, which may have been generated due to the oxidization treatments that may probably have provoked micropores widening. Interestingly, it is remarked that this pores' region is more prominent in Air. H_2O.Pl, compared to Hox.

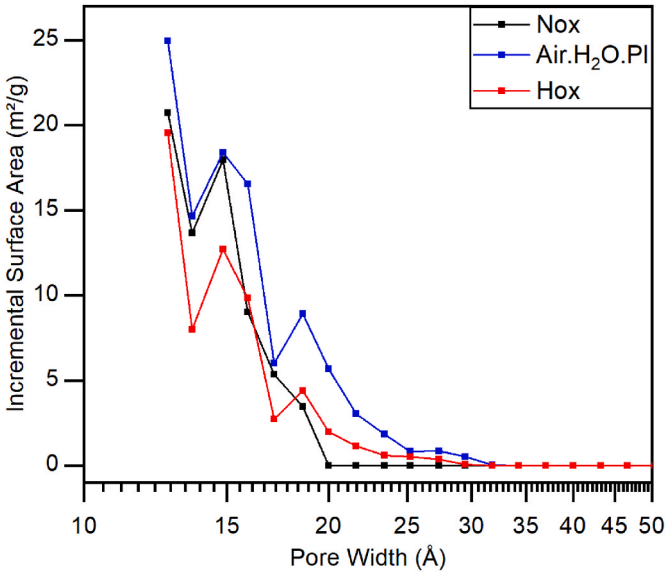

Fig. 13. DFT pores' distribution of non-oxidized (Nox) and oxidized carbons (Hox, Air. H_2O.Pl).

Little research has been done on activated carbon oxidation with plasma and their possible morphological changes after plasma exposure. For this reason, SEM imaging was carried out on three activated carbon samples (Nox, Hox and Air. H_2O.Pl) and indeed, different textures are observed, depending on their oxidation treatment. As can be observed in Fig. 14, while no visible pores are seen in Nox, after contacting HNO_3, several pores of different diameters are created and an irregular general texture is observed in the material. In comparison, the sample treated with plasma is notably smoother, though pores of around 1 μm spaced in a really regular pattern are evidenced throughout all the carbon surface.

3.2.5. *Final overview of the applied oxidation methods*

Table 3 give a summarized overview of all the methods applied in this research, their main findings and the main advantage of each one. This highlights the benefits of using plasma as functionalization procedure for granular activated carbons.

4. Conclusions

Granular activated carbon has been oxidized by the wet-chemistry and plasma approaches in a comparative manner. Regarding the wet-chemistry approach, HNO_3 oxidation attained high oxidation

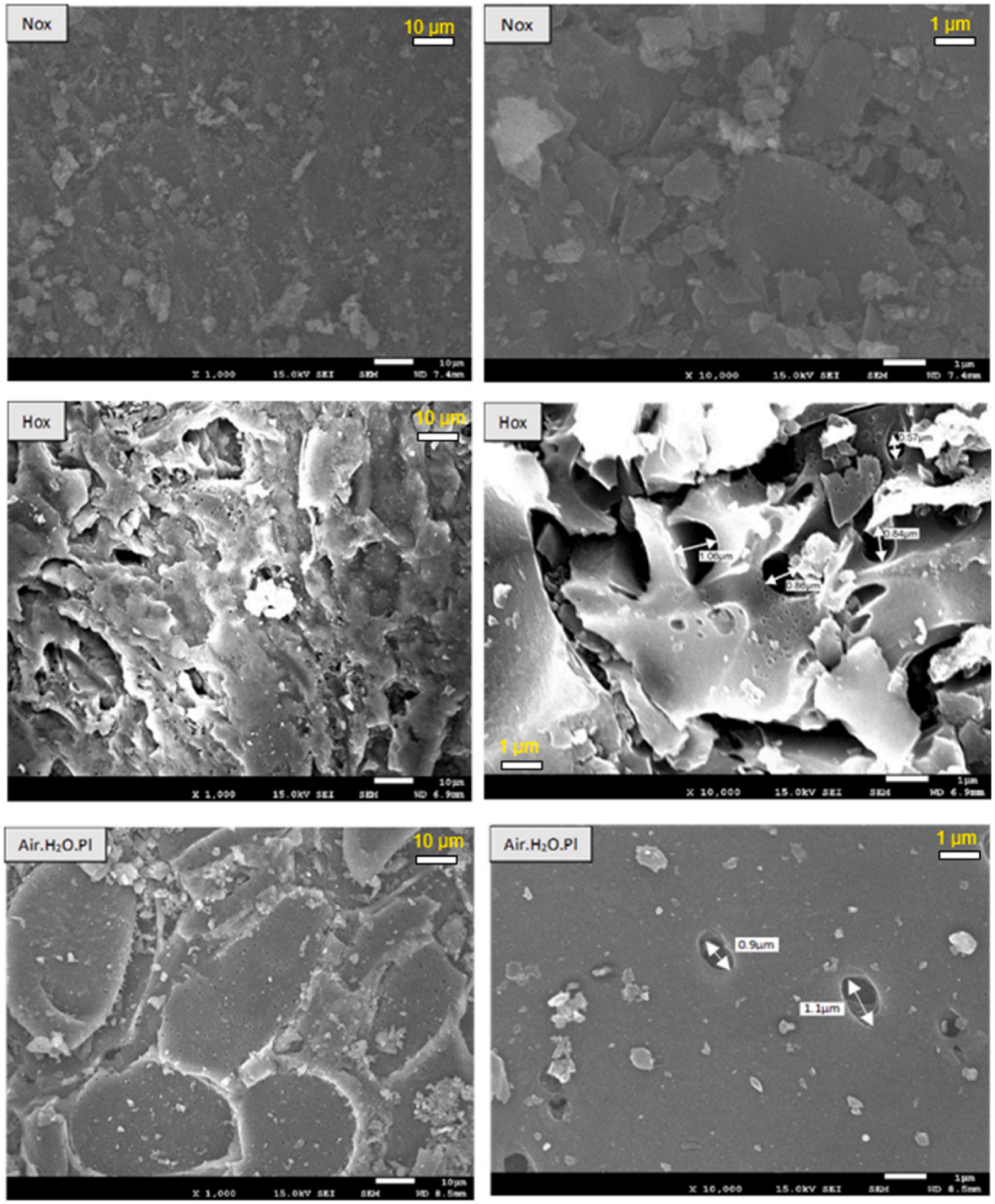

Fig. 14. SEM images of non-oxidized (Nox), and oxidized activated carbons (Hox and Air. H_2O.Pl). Scales bars are: 10 μm (left column) and 1 μm (right column).

Table 3
Summary of results- Wet chemistry vs Plasma approach.

Oxidation Method	Type	Treatment details	Main advantage	O–C/Total C by XPS	Total acidity (mmol/100 g) by Boehm	Main functional group by Boehm
Non- oxidized (pristine)	–	–	–	0.09	8	Lactones
Wet chemistry	HNO_3	6 h, 4 g, HNO_3 2.5 M	Traditional method. No need of sophisticated equipment	0.23	156	Carboxylic acids
	H_2O_2	10 h, 4 g, H_2O_2 35 %		0.18	77	Phenols
Plasma	Suspension mode	O_2 plasma (90 min,1.5 g AC)	Rapid method, generation of H_2O_2 in-situ	–	57	Phenols
	Solid mode		Rapid method, solvent-free, reagent-free, no post- treatment (washing, drying)	–	205	Carboxylic acids
		Air plasma (90 min, 6 g)		0.17	98	
		Air. H_2O. plasma (90 min, 6 g)		0.19	118	
		O_2 plasma (90 min, 6 g)		0.16	102	
		O_2. H_2O. plasma (90 min, 6 g)		0.18	100	

efficiency characterized by an important presence of surface carboxylic acid groups. In contrast, H_2O_2 oxidation gave lower oxidation efficiency with a predominant existence of phenol functionalities. In comparison, plasma was found capable of oxidizing the material at different degrees, with different type of functional groups, depending on the way in which it was exposed to plasma and the time of treatment. If the carbon granules were exposed directly to the plasma plume (in *solid mode*), the material obtained a high oxidation degree, with carboxylic acid groups as the main oxygen functionality, showing similar characteristics as HNO_3 oxidized carbon in the wet-chemistry approach. In this case, the carbon's oxidation was most probably caused due to HNO_3 plasma generated species. In contrast, if the activated carbon grains were exposed to the plasma plume while being suspended in water *(suspension mode)*, the oxidation degree was milder and phenols were found to be the most abundant functionality, similarly to H_2O_2 oxidized activated carbon. In this case, H_2O_2 plasma generated species in solution may have been the main agent that caused carbon's oxidation. Furthermore, it was demonstrated that while oxidizing the carbon in the *solid mode*, changing the type of gas source for plasma generation had little influence on the oxidation degree of the sample and the type of oxygen functional groups created, being in all cases carboxylic acid groups the most abundant oxygen functionality. Moreover, the material reached a "saturation point" and could no longer increase its oxidation degree after a certain duration, while the majority of oxidized functions were introduced at short exposure periods (30 min). Nevertheless, the samples oxidized by dry gases contained a higher amount of nitrates/nitrites, while the ones oxidized by humidified gases showed FTIR bands and XPS oxygen contents that may denote a higher presence of O–H containing species in the carbon after its plasma exposure. Stability tests showed that the acidic functions introduced by plasma seem stable for at least 6 weeks, where no new oxygen functions seemed to have been incorporated, neither removed during this tested time. Finally, activated carbon oxidation decreased the material's surface area and microporous volume in all the tested approaches, nevertheless, plasma oxidation impacted the solid in a notably milder way, while creating a smoother surface and regular-patterned ≈1 μm pores. All in all, Glidarc plasma technology is a versatile and interesting tool for activated carbon functionalization that permits the oxidation of the solid in a rapid, solvent-free way, with good oxidation efficiency and with the possibility to tune the type of desired oxygen functionality, by varying the way in which the carbon is exposed to the plasma plume. Moreover, thanks to its characteristics, this oxidation method could have good scale-up perspectives that may allow the functionalization of activated carbon in a greener way than the traditional wet-chemistry approach, characterized by the use of dangerous substances, high temperatures and long, multi-step reactions that need time-consuming washing and drying steps and generating highly acidic waste.

In future research, it would be valuable to further investigate the reactions that occur in the material immediately after plasma exposure. This could provide deeper fundamental insights into the plasma oxidation reactions with air and oxygen in carbon, enhancing our understanding of the oxidation mechanism of carbon with Glidarc-plasma and potentially further optimizing it. Additionally, it would be interesting to explore how carbon morphology influences the formation and stability of oxygen species through plasma functionalization. Therefore, the oxidation of other carbon materials, such as carbon black, carbon nanotubes, and graphite, could be tested applying the same methodology and expanding it.

CRediT authorship contribution statement

Nathalie de la Torre-Miranda: Writing – review & editing, Writing – original draft, Visualization, Methodology, Investigation, Formal analysis, Conceptualization. **Pierre Eloy:** Formal analysis, Data curation. **Eric M. Gaigneaux:** Resources, Conceptualization. **Sophie Hermans:** Writing – review & editing, Supervision, Resources, Project administration, Funding acquisition, Conceptualization.

Declaration of competing interest

The authors declare that they have no known competing financial interests or personal relationships that could have appeared to influence the work reported in this paper.

Acknowledgements

The authors are thankful to Conseil d'Action International (CAI) and ARES scholarship programs for funding this research. We thank Jean François Statsyns, Francois Devred and Delphine Magnin for their constant technical support and help. We are grateful to Departamento de Metalurgia Extractiva (DEMEX) from Escuela Politécnica Nacional in Quito, Ecuador, for supplying the non-functionalized granular Calgon carbon and for the technical cooperation between our institutions.

Appendix A. Supplementary data

Supplementary data to this article can be found online at https://doi.org/10.1016/j.matchemphys.2025.130878.

Data availability

Data will be made available on request.

References

[1] Deborah Chung, Carbon Materials, Science and applications, Engineering Materials for Technological Needs, New York 3 (2019).

[2] C.Y. Yin, M.K. Aroua, W.M.A.W. Daud, Review of modifications of activated carbon for enhancing contaminant uptakes from aqueous solutions, Sep. Purif. Technol. 52 (2007) 403–415, https://doi.org/10.1016/j.seppur.2006.06.009.

[3] F. Rodríguez-Reinoso, Activated carbon and adsorption, in: P.V.K.H. Jürgen Buschow, Robert W. Cahn, Merton C. Flemings, Bernhard Ilschner, Edward J. Kramer, Subhash Mahajan (Eds.), Encycl. Mater. Sci. Technol., Elsevier, 2001, pp. 22–34, https://doi.org/10.1016/B0-08-043152-6/00005-X.

[4] H. Marsh, F. Rodriguez-Reinoso, Activated Carbon, first ed., Elsevier Ltd, Great Britain, 2006.

[5] W.M.A.W. Daud, A.H. Houshamnd, Textural characteristics, surface chemistry and oxidation of activated carbon, J. Nat. Gas Chem. 19 (2010) 267–279, https://doi.org/10.1016/S1003-9953(09)60066-9.

[6] M. Mariana, A.K. Abdul, E.M. Mistar, E.B. Yahya, T. Alfatah, M. Danish, M. Amayreh, Recent advances in activated carbon modification techniques for enhanced heavy metal adsorption, J. Water Process Eng. 43 (2021) 102221, https://doi.org/10.1016/j.jwpe.2021.102221.

[7] X. Yang, Y. Wan, Y. Zheng, F. He, Z. Yu, J. Huang, H. Wang, Y.S. Ok, Y. Jiang, B. Gao, Surface functional groups of carbon-based adsorbents and their roles in the removal of heavy metals from aqueous solutions: a critical review, Chem. Eng. J. 366 (2019) 608–621, https://doi.org/10.1016/j.cej.2019.02.119.

[8] J. Rivera-Utrilla, M. Sánchez-Polo, V. Gómez-Serrano, P.M. Álvarez, M.C.M. Alvim-Ferraz, J.M. Dias, Activated carbon modifications to enhance its water treatment applications. An overview, J. Hazard Mater. 187 (2011) 1–23, https://doi.org/10.1016/j.jhazmat.2011.01.033.

[9] P. Chingombe, B. Saha, R.J. Wakeman, Surface modification and characterisation of a coal-based activated carbon, Carbon N. Y. 43 (2005) 3132–3143, https://doi.org/10.1016/j.carbon.2005.06.021.

[10] H.P. Boehm, Some aspects of the surface chemistry of carbon blacks and other carbons, Carbon N. Y. 32 (1994) 759–769, https://doi.org/10.1016/0008-6223(94)90031-0.

[11] H.P. Boehm, Surface oxides on carbon and their analysis: a critical assessment, Carbon N. Y. 40 (2002) 145–149, https://doi.org/10.1016/S0008-6223(01)00165-8.

[12] W. Shen, W. Fan, Nitrogen-containing porous carbons: synthesis and application, J. Mater. Chem. A 1 (2013) 999–1013, https://doi.org/10.1039/c2ta00028h.

[13] R. Zanella, E.V. Basiuk, P. Santiago, V.A. Basiuk, E. Mireles, I. Puente-Lee, J. M. Saniger, Deposition of gold nanoparticles onto thiol-functionalized multiwalled carbon nanotubes, J. Phys. Chem. B 109 (2005) 16290–16295, https://doi.org/10.1021/jp0521454.

[14] V. Basiuk, E. Basiuk, Chemical derivatization of carbon nanotube tips, in: H. S. Nalwa (Ed.), Encycl. Nanosci. Nanotechnol., American Scientific Publishers, California, 2004, pp. 761–776.

[15] D. Vidick, A.F. Leonard, C. Poleunis, A. Delcorte, M. Devillers, S. Hermans, Phosphine- and ammonium-functionalized ordered mesoporous carbons as supports for cluster-derived metal nanoparticles, Catal. Today 235 (2014) 112–126, https://doi.org/10.1016/j.cattod.2014.03.017.

[16] A. Alam, C. Wan, T. McNally, Surface amination of carbon nanoparticles for modification of epoxy resins: plasma-treatment vs. wet-chemistry approach, Eur. Polym. J. 87 (2017) 422–448, https://doi.org/10.1016/j.eurpolymj.2016.10.004.

[17] S. Hermans, V. Bruyr, M. Devillers, A templating effect of carbon nanomaterials on the synthesis of Pd nanoparticles by covalent grafting onto surface O-groups, J. Mater. Chem. 22 (2012) 14479–14486, https://doi.org/10.1039/c2jm31027a.

[18] J.L. Figueiredo, M.F.R. Pereira, M.M.A. Freitas, J.J.M. Órfão, Modification of the surface chemistry of activated carbons, Carbon N. Y. 37 (1999) 1379–1389, https://doi.org/10.1016/S0008-6223(98)00333-9.

[19] C. Moreno-Castilla, M.V. López-Ramón, F. Carrasco-Marín, Changes in surface chemistry of activated carbons by wet oxidation, Carbon N. Y. 38 (2000) 1995–2001, https://doi.org/10.1016/S0008-6223(00)00048-8.

[20] A. Merenda, E. Des Ligneris, K. Sears, T. Chaffraix, K. Magniez, D. Cornu, J. A. Schütz, L.F. Dumée, Assessing the temporal stability of surface functional groups introduced by plasma treatments on the outer shells of carbon nanotubes, Sci. Rep. 6 (2016) 1–12, https://doi.org/10.1038/srep31565.

[21] C.O. Ania, J.B. Parra, J.J. Pis, Influence of oxygen-containing functional groups on active carbon adsorption of selected organic compounds, Fuel Process. Technol. 79 (2002) 265–271, https://doi.org/10.1016/S0378-3820(02)00184-4.

[22] W. Qiao, Y. Korai, I. Mochida, Y. Hori, T. Maeda, Preparation of an activated carbon artifact: oxidative modification of coconut shell-based carbon to improve the strength, Carbon N. Y. 40 (2002) 351–358, https://doi.org/10.1016/S0008-6223(01)00110-5.

[23] J.-L. Brisset, E. Hnatiuc, Peroxynitrite: a Re-examination of the chemical properties of non-thermal discharges burning in air over aqueous solutions, Plasma Chem. Plasma Process. 32 (2012) 655–674, https://doi.org/10.1007/s11090-012-9384-x.

[24] J.P. Boudou, J.I. Paredes, A. Cuesta, A. Martínez-Alonso, J.M.D. Tascón, Oxygen plasma modification of pitch-based isotropic carbon fibres, Carbon N. Y. 41 (2003) 41–56, https://doi.org/10.1016/S0008-6223(02)00270-1.

[25] A. Tiya-Djowe, M.A. Dourges, J.L. Bruneel, H. Deleuze, Plasma-deposition of α-FeOOH particles on biochar using a gliding arc discharge in humid air: a green and sustainable route for producing oxidation catalysts, RSC Adv. 9 (2019) 4797–4805, https://doi.org/10.1039/c9ra00671k.

[26] B. Sop Tamo, G. Kamgang-Youbi, E. Acayanka, L. Medjo Simo, A. Tiya-Djowe, D. Kuete-Saa, S. Laminsi, L. Tchadjie, Plasma chemical functionalisation of a Cameroonian kaolinite clay for a greater hydrophilicity, Plasma Chem. Plasma Process. 36 (2016) 1449–1469, https://doi.org/10.1007/s11090-016-9731-4.

[27] A.B. García, A. Martínez-Alonso, C.A. Leon Y Leon, J.M.D. Tascón, Modification of the surface properties of an activated carbon by oxygen plasma treatment, Fuel 77 (1998) 613–624, https://doi.org/10.1016/S0016-2361(97)00111-7.

[28] M. Domingo-García, F.J. López-Garzón, M. Pérez-Mendoza, Effect of some oxidation treatments on the textural characteristics and surface chemical nature of an activated carbon, J. Colloid Interface Sci. 222 (2000) 233–240, https://doi.org/10.1006/jcis.1999.6619.

[29] A. Felten, C. Bittencourt, J.J. Pireaux, G. Van Lier, J.C. Charlier, Radio-frequency plasma functionalization of carbon nanotubes surface O_2, NH_3, and CF_4 treatments, J. Appl. Phys. 98 (2005), https://doi.org/10.1063/1.2071455.

[30] Y. Huang, Q. Yu, M. Li, S. Jin, J. Fan, L. Zhao, Z. Yao, Surface modification of activated carbon fiber by low-temperature oxygen plasma: textural property, surface chemistry, and the effect of water vapor adsorption, Chem. Eng. J. 418 (2021) 129474, https://doi.org/10.1016/j.cej.2021.129474.

[31] D. Lee, S.H. Hong, K.H. Paek, W.T. Ju, Adsorbability enhancement of activated carbon by dielectric barrier discharge plasma treatment, Surf. Coating. Technol. 200 (2005) 2277–2282, https://doi.org/10.1016/j.surfcoat.2004.11.027.

[32] C.M. Du, D.W. Huang, H.X. Li, M.D. Xiao, K. Wang, L. Zhang, Z.Y. Li, T.F. Chen, J. M. Mo, D. Gao, Y.H. Huang, S.K. Liu, L. Yu, C.R. Zhang, Adsorption of acid Orange II from aqueous solution by plasma modified activated carbon fibers, Plasma Chem. Plasma Process. 33 (2013) 65–82, https://doi.org/10.1007/s11090-012-9412-x.

[33] A. Czernichowski, Gliding arc. Applications to engineering and environment control, Pure Appl. Chem. 66 (1994) 1301–1310, https://doi.org/10.1351/pac199466061301.

[34] F.W.B. Tatchemo, S. Nzali, G. Kamgang Youbi, A. Tiya Djowe, D.K. Saa, E. Acayanka, S. Laminsi, E.M. Gaigneaux, Gliding arc plasma synthesis of MnO2 nanorods for the plasma-catalytic bleaching of azoïc amaranth red dye, Top. Catal. 60 (2017) 962–972, https://doi.org/10.1007/s11244-017-0761-9.

[35] F.W. Boyom-Tatchemo, F. Devred, G. Ndiffo-Yemeli, S. Laminsi, E.M. Gaigneaux, Plasma-induced redox reactions synthesis of nanosized α-, γ- and δ-MnO2 catalysts for dye degradation, Appl. Catal. B Environ. 260 (2020), https://doi.org/10.1016/j.apcatb.2019.118159.

[36] J. Rouquerol, P. Llewellyn, F. Rouquerol, Is the BET equation applicable to microporous adsorbents? in: N.S.P.L. Llewellyn, F. Rodriquez-Reinoso (Eds.), Stud. Surf. Sci. Catal. Elsevier B.V., 2007, pp. 49–56. J.R.

[37] F. Rouquerol, L. Luciani, P. Llewellyn, R. Denoyel, J. Rouquerol, Texture des matériaux pulvérulents ou poreux, Tech. l'ingenieur 1050 (1) (2003), https://doi.org/10.51257/a-v3-p1050, 1050_24.

[38] H.P. Boehm, Chemical identification of surface groups, Adv. Catal. 16 (1966) 179–274, https://doi.org/10.1016/S0360-0564(08)60354-5.

[39] A.C. Tarasuk, H.A. Andreas, A.M. Oickle, S.L. Goertzen, K.D. Thériault, Standardization of the boehm titration. Part I. CO2 expulsion and endpoint determination, Carbon N. Y. 48 (2009) 1252–1261, https://doi.org/10.1016/j.carbon.2009.11.050.

[40] Y.O. Abdalla, A.M. Oickle, H.A. Andreas, K.R. Hopper, S.L. Goertzen, Standardization of the boehm titration: part II. Method of agitation, effect of filtering and dilute titrant, Carbon N. Y. 48 (2010) 3313–3322, https://doi.org/10.1016/j.carbon.2010.05.004.

[41] H. Lesueur, A. Czernichowski, J. Chapelle, A device for the formation of low temperature plasma by means of glidng electric discharges 2 (639) (1988) 172.

[42] S. Hermans, C. Diverchy, O. Demoulin, V. Dubois, E.M. Gaigneaux, M. Devillers, Nanostructured Pd/C catalysts prepared by grafting of model carboxylate complexes onto functionalized carbon, J. Catal. 243 (2006) 239–251, https://doi.org/10.1016/j.jcat.2006.07.019.

[43] I.I. Salame, T.J. Bandosz, Surface chemistry of activated carbons: combining the results of temperature-programmed desorption, boehm, and potentiometric titrations, J. Colloid Interface Sci. 240 (2001) 252–258, https://doi.org/10.1006/jcis.2001.7596.

[44] C. Moreno-Castilla, M.A. Ferro-García, J.P. Joly, I. Bautista-Toledo, F. Carrasco-Marín, J. Rivera-Utrilla, Activated carbon surface modifications by nitric acid, hydrogen peroxide, and ammonium peroxydisulfate treatments, Langmuir 11 (1995) 4386–4392, https://doi.org/10.1021/la00011a035.

[45] S. Afreen, K. Kokubo, K. Muthoosamy, S. Manickam, Hydration or hydroxylation: direct synthesis of fullerenol from pristine fullerene [C60] via acoustic cavitation in the presence of hydrogen peroxide, RSC Adv. 7 (2017) 31930–31939, https://doi.org/10.1039/c7ra03799f.

[46] C. Moreno-Castilla, M.A. Ferro-García, J.P. Joly, I. Bautista-Toledo, F. Carrasco-Marín, J. Rivera-Utrilla, Activated carbon surface modifications by nitric acid, hydrogen peroxide, and ammonium peroxydisulfate treatmenss, Langmuir 11 (1995) 4386–4392, https://doi.org/10.1021/la00011a035.

[47] S. Shin, J. Jang, S.H. Yoon, I. Mochida, A study on the effect of heat treatment on functional groups of pitch based activated carbon fiber using FTIR, Carbon N. Y. 35 (1997) 1739–1743, https://doi.org/10.1016/S0008-6223(97)00132-2.

[48] G. Socrates, Infrared and Raman Characteristic Group Frequencies, third ed., John Wiley & Sons Ltd., England, 2001.

[49] P.E. Fanning, M.A. Vannice, A DRIFTS study of the formation of surface groups on carbon by oxidation, Carbon N. Y. 31 (1993) 721–730, https://doi.org/10.1016/0008-6223(93)90009-Y.

[50] NIST X-ray Photoelectron Spectroscopy Databas, NIST X-ray photoelectron spectroscopy database, NIST Stand, Ref, 2000, https://doi.org/10.18434/T4T88K.

[51] S. Aduru, S. Contarini, J.W. Rabalais, Electron-, X-ray-, and ion-stimulated decomposition, J. Phys. Chem. 90 (1986) 1683–1688.

[52] B. Stöhr, H.P. Boehm, R. Schlögl, Enhancement of the catalytic activity of activated carbons in oxidation reactions by thermal treatment with ammonia or hydrogen

cyanide and observation of a superoxide species as a possible intermediate, Carbon N. Y. 29 (1991) 707–720, https://doi.org/10.1016/0008-6223(91)90006-5.
[53] S.R. Kelemen, M. Afeworki, M.L. Gorbaty, P.J. Kwiatek, M.S. Solum, J.Z. Hu, R. J. Pugmire, XPS and 15N NMR study of nitrogen forms in carbonaceous solids, Energy Fuels 16 (2002) 1507–1515, https://doi.org/10.1021/ef0200828.
[54] J.S. Stevens, S.J. Byard, C.A. Muryn, S.L.M. Schroeder, Identification of protonation state by XPS, solid-state NMR, and DFT: characterization of the nature of a new theophylline complex by experimental and computational methods, J. Phys. Chem. B 114 (2010) 13961–13969, https://doi.org/10.1021/jp106465u.
[55] H.K. Shin, M. Park, H.Y. Kim, S.J. Park, An overview of new oxidation methods for polyacrylonitrile-based carbon fibers, Carbon Lett. 16 (2015) 11–18, https://doi.org/10.5714/CL.2015.16.1.011.
[56] S. O'Kell, T. Henshaw, G. Farrow, M. Aindow, C. Jones, Effects of low-power plasma treatment on polyethylene surfaces, Surf. Interface Anal. 23 (1995) 319–327, https://doi.org/10.1002/sia.740230508.
[57] J. Boudou, J. Paredes, A. Cuesta, A. Martinez- Alonso, J. Tascón, Oxygen plasma modification of pitch-based isotropic carbon fibres, Carbon N. Y. 41 (2003) 41–56.
[58] M.C. Paiva, C.A. Bernardo, M. Nardin, Mechanical, surface and interfacial characterization of pitch and PAN-Based carbon fibres, Carbon N. Y. 38 (2000) 1323–1337, https://doi.org/10.1016/S0008-6223(99)00266-3.
[59] B. Benstaali, P. Boubert, B.G. Cheron, A. Addou, J.L. Brisset, Density and rotational temperature measurements of the OH° and NO° radicals produced by a gliding arc in humid air, Plasma Chem. Plasma Process. 22 (2002) 553–571, https://doi.org/10.1023/A:1021371529955.
[60] D. Porter, M.D. Poplin, F. Holzer, W.C. Finney, B.R. Locke, Formation of hydrogen peroxide, hydrogen, and oxygen in gliding arc electrical discharge reactors with water spray, IEEE Trans. Ind. Appl. 45 (2009) 623–629, https://doi.org/10.1109/TIA.2009.2013560.
[61] R. Burlica, K.Y. Shih, B.R. Locke, Formation of H2and H2O2in a water-spray gliding arc nonthermal plasma reactor, Ind. Eng. Chem. Res. 49 (2010) 6342–6349, https://doi.org/10.1021/ie100038g.
[62] R. Burlica, R.G. Grim, K.Y. Shih, D. Balkwill, B.R. Locke, Bacteria inactivation using low power pulsed gliding arc discharges with water spray, Plasma Process. Polym. 7 (2010) 640–649, https://doi.org/10.1002/ppap.200900183.
[63] R. Foerch, N.S. Mcintyre, R.N.S. Sodhi, D.H. Hunter, Nitrogen plasma treatment of polyethylene and polystyrene in a remote plasma reactor, J. Appl. Polym. Sci. 40 (1990) 1903–1915, https://doi.org/10.1002/app.1990.070401109.
[64] S. Hussain, R. Amade, E. Jover, E. Bertran, Nitrogen plasma functionalization of carbon nanotubes for supercapacitor applications, J. Mater. Sci. 48 (2013) 7620–7628, https://doi.org/10.1007/s10853-013-7579-z.
[65] G.S. Szymański, Z. Karpiński, S. Biniak, A. Świątkowski, The effect of the gradual thermal decomposition of surface oxygen species on the chemical and catalytic properties of oxidized activated carbon, Carbon N. Y. 40 (2002) 2627–2639, https://doi.org/10.1016/S0008-6223(02)00188-4.
[66] R.R.A. Rios, D.E. Alves, I. Dalmázio, S.F.V. Bento, C.L. Donnici, R.M. Lago, Tailoring activated carbon by surface chemical modification with O, S, and N containing molecules, Mater. Res. 6 (2003) 129–135, https://doi.org/10.1590/s1516-14392003000200004.
[67] M.M. Maroto-Valer, I. Dranca, T. Lupascu, R. Nastas, Effect of adsorbate polarity on thermodesorption profiles from oxidized and metal-impregnated activated carbons, Carbon N. Y. 42 (2004) 2655–2659, https://doi.org/10.1016/j.carbon.2004.06.007.
[68] B. Ruelle, S. Peeterbroeck, T. Godfroid, C. Bittencourt, M. Hecq, R. Snyders, P. Dubois, Selective grafting of primary amines onto carbon nanotubes via free-radical treatment in microwave plasma post-discharge, Polymers 4 (2012) 296–315, https://doi.org/10.3390/polym4010296.
[69] K.S.W. Sing, R.T. Williams, Physisorption hysteresis loops and the characterization of nanoporous materials, Adsorpt. Sci. Technol. 22 (2004) 773–782, https://doi.org/10.1260/0263617053499032.
[70] N. Fairley, et al., Systematic and collaborative approach to problem solving using X-ray photoelectron spectroscopy, Applied Surface Science Advances (2021), https://doi.org/10.1016/j.apsadv.2021.100112.
[71] F. Hanon, S. Hermans, E.M. Gaigneaux, What are the species involved in the gliding arc plasma synthesis of heterogeneous catalysts? Catal. Today 430 (2024) 114550.